

Reviewer #1

Dear Editor Dr. Yin and Anonymous Reviewers:

We really appreciate your time and efforts that you have spent in reading, reviewing and handling our manuscript. Your comments and suggestions have greatly improved our manuscript. Following these insightful comments and suggestions, we have conducted a point-to-point revision as listed below. We have reproduced the reviewers' comments in blue fonts, and our responses in black fonts directly below the comments. We hope that our revised manuscript is now considered to be suitable for publication with your high standard journal.

Main Comments:

1. The speleothem oxygen-isotope has high resolution, thus, its upward or downward trends over some specific time periods need to be quantified using the trend test methods e.g. Mann-Kendall non-parametric trend test. Moreover, the magnitude and amplitude of the EASM intensity also need to be calculated.

Reply: Many thanks for your suggestion. The upward trend during the MCA has been constrained through a linear fit method in the stalagmite $\delta^{18}\text{O}$ record and other climatic reconstructions (see new Fig. 4) in the revised manuscript. The magnitude and amplitude of the stalagmite $\delta^{18}\text{O}$ records have not been calculated. This is because the strength of MCA, LIA and CWP is not globally coherent, and in addition, our Yongxing record does not span the whole MCA and CWP periods. Most importantly, stalagmite $\delta^{18}\text{O}$ records in each cave do not have the same absolute values over the same period and their fluctuations are not coherent as well because of the different rainfall mixing extent in the epikarst zone.

2. According to the background of the co-authors, a more mechanism of EASM variation should be discussed. e.g. how the NAO effects the East Asian summer monsoon, based on some instrumental datasets or CMIP5 datasets.

Reply: Thanks a lot for pointing out this. More mechanisms of EASM variation have been added based on some instrumental datasets. We have added the following text in our revised manuscript: "An analysis of instrumental data indicates that the winter NAO signal can be transmitted to East Asia through a wave train bridge and leads to a drier southern China but slightly wetter central China (Sung et al., 2006). On the other hand, Wu et al. (2009) have proposed that NAO-related spring SST anomalies in the North Atlantic can produce anomalous anticyclonic circulations over the Okhotsk Sea, which help to enhance the subtropical monsoon front."

3. The other proxy reconstruction from tree-ring [Liu et al., 2019] and historical documentary [Ge et al., 2008] are suggested to cross check the speleothem EASM reconstruction. Moreover, a detailed and independent local temperature reconstruction should be used to explore the relationship between the speleothem oxygen-isotope and the temperature, e.g. [Cook et al., 2013; Shi et al., 2015; Zhang et al., 2018].

Reply: The other proxy reconstructions from tree-ring (Liu et al., 2019) and historical document (Ge et al., 2009) have been utilized to cross check the speleothem $\delta^{18}\text{O}$ record. Moreover, local temperature reconstructions have been utilized to make a comparison with our stalagmite $\delta^{18}\text{O}$ record. However, our stalagmite $\delta^{18}\text{O}$ record does not show a significant correlation with these

climatic reconstructions (see Figs. 1 and 2 below in our response).

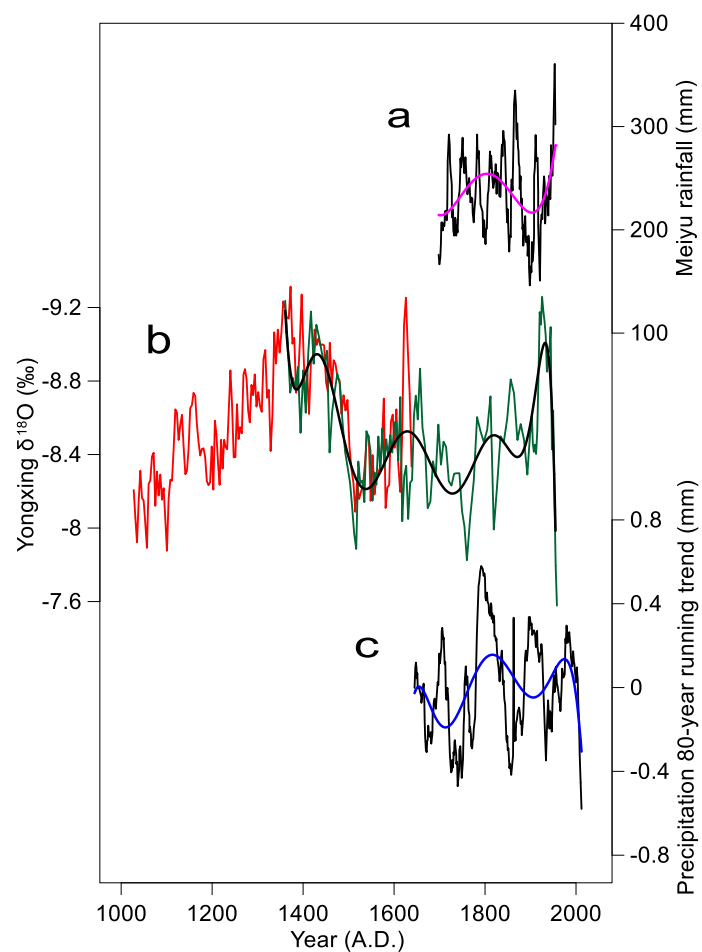


Fig. 1 Comparisons of the Yongxing $\delta^{18}\text{O}$ record with other proxy reconstructions. (a) Meiyu rain from historical documents (Ge et al., 2008); (b) Yongxing $\delta^{18}\text{O}$ record (this study); (c) Precipitation reconstruction from tree-ring (Liu et al., 2019).

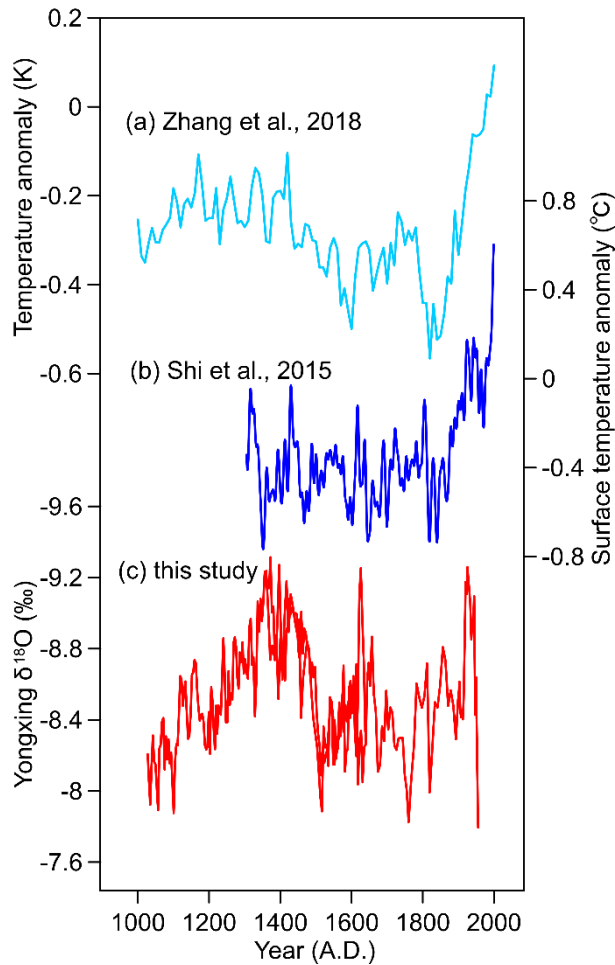


Fig. 2 Comparison of (c) the Yongxing $\delta^{18}\text{O}$ record and temperature reconstructions by (a) Zhang et al., 2018 and (b) Shi et al., 2015.

Specific Comments:

1. Page 1, Lines 25-26. What meaning is the 'EASM intensity'? the amplitude or magnitude of the EASM variation?

Reply: The EASM intensity means the magnitude of the EASM itself. Based on a recent study of Zhang et al., (2018), we have rephrased the “EASM intensity” to Meiyu rain in our revised manuscript.

2. Page 2, Line 49. It is 'Mann'. Moreover, Chen (2018) is not the temperature reconstruction.

Reply: Many thanks for your corrections, we have changed ‘Man’ to ‘Mann’ and deleted ‘Chen (2018)’ in our revised manuscript.

3. Page 2, Lines 63-67. The detained review about the disagreement of the influence ENSO on EASM is very interesting and suggested to help the following analysis.

Reply: Many thanks for your positive comments here.

4. Page 3, Lines 78-79. The 'direct evidence' is not rigorous, even it is still difficult to connect the AMOC and EASM for the instrumental dataset analysis.

Reply: Thank you for your comments. We have revised the original expression as “available empirical data is still rare to explore the potential link between the AMOC and regional precipitation during the MCA and LIA intervals” in our revised manuscript.

5. Page 4, Lines 132-133. There is a large discrepancy between YX262 and YX275 in the early 1600s. A discussion of this difference is suggested to indicate a stable condition of the isotope.

Reply: Thank for your suggestion. We have added some discussion as follows: “A minor difference exists between the two stalagmite $\delta^{18}\text{O}$ records. The YX262 record shows a larger shift toward more negative values than the YX275 record in the early 1600s. Different feeding systems for both the stalagmites probably produce the $\delta^{18}\text{O}$ discrepancy. Longer mixing of meteorological rain within the overlying bedrock may dampen the overall rain $\delta^{18}\text{O}$ amplitude and therefore lead to the calcite $\delta^{18}\text{O}$ offsets (Tan et al., 2019; Carolin et al., 2013). Overall, the good replication between the two records suggests that the YX262 $\delta^{18}\text{O}$ signal is less influenced by the kinetic fractionation and is primarily of climatic origin.” in our revised manuscript.

6. Page 5, Lines 141-142. The EASM intensity is not equal to the local rainfall, e.g. the increasing meiyu rainfall means the weak EASM.

Reply: Thank you for your suggestion. We have revised this inaccurate expression. ‘the EASM intensity’ has been revised as ‘Meiyu rain’.

7. Page 6. Lines 188-189. The statement is inaccurate, since the north-drought and south-flood can be affected by the same factor from the instrumental analysis.

Reply: Thanks for your comment. We suggest that the north drought and south flood could result from meridional migration of the Meiyu rain belt (Yu and Zhou., 2007; Zhou et al., 2009; Zhang et al., 2018). We have added this statement in our revised manuscript.

8. Page 7, Lines 214-215. In fact, the EASM becomes weak since the late 1970s [Wang, 2001].

Reply: The EASM shows remarkable multi-decadal variability during the 20th century. The weakening of the EASM since the late 1970s attracts wide attention (Wang., 2001; Zhou et al., 2009). Recently, it is suggested that the EASM has been recovering since the early 1990s (Liu et al., 2012). Here our stalagmite record shows that the EASM increase step by step since the end of LIA on the centennial scale, generally in agreement with the increasing tendency of the global temperature. We interpret the weakening of the EASM between 1970s-1990s as a portion of the EASM multi-decadal variability, which punctuated the centennial EASM increasing since the LIA.

9. Pages 7-8. Lines 229-235. When you check Walker cell, the position of ascending or sinking branch is also important for atmosphere transport.

Reply: Thank you for your suggestion. We have considered your comments here in our revised manuscript.

10. Pages 9-10, Lines 278-311. The relationship between NAO and EASM during the CWP is complex, why it is stable during the LIA or MCA. Is a possible reason the uncertainty of NAO reconstruction?

Reply: The correlation seems better between the NAO and EASM over the MCA and LIA than the

CWP. For example, a maximum monsoon rainfall centered at 1900AD corresponds to a more negative NAO index, contradicting to the relationship between them over the MCA and LIA. The proxy-based NAO index (Trouet et al., 2009) used in the context can be consolidated by the instrumental NAO index series (Jones et al., 1997). The varied relationship over the CWP may depend on timescales as well. A better relationship occurs on centennial scales, rather than on decadal or shorter timescales.

References

- Carolin S. A. et al., Varied response of western Pacific hydrology to climate forcings over the last glacial period. *Science*, 340, 1564–1566, 2013.
- Cobb, K. M., Charles, C. D., Cheng, H. & Edwards, R. L. El Nino/Southern Oscillation and tropical Pacific climate during the last millennium, *Nature*, 424, 271–276, 2003.
- Ge, Q., Guo, X., Zheng, J., Hao, Z.: Meiyu in the middle and lower reaches of the Yangtze River since 1736, *Chinese Sci. Bull.*, 53, 107-114, 2008.
- Graham, N. E. et al. Tropical Pacific—mid-latitude teleconnections in medieval times. *Clim. Change*, 83, 241–285, 2007.
- Jones, P., Jonsson, T., Wheeler, D.: Extension to the North Atlantic oscillation using early instrumental pressure observations from Gibraltar and south-west Iceland, *Int. J. Climatol.*, 17, 1433-1450, 1997.
- Liu, H., Zhou, T., Zhu, Y., Lin, Y.: The strengthening East Asian summer monsoon since the early 1990s, *Chinese Sci. Bull.*, 57, 1553-1558, 2012.
- Liu, Y., Cai, W., Sun, C., Song, H., Cobb, K., Li, J., Leavitt, S., Wu, L., Cai, Q., Liu, R., Ng, B., Cherubini, P., Büentgen, U., Song, Y., Wang, G., Lei, Y., Yan, L., Li, Q., Ma, Y., Fang, C., Sun, J., Li, X., Chen, D., Linderholm, H.: Anthropogenic aerosols cause recent pronounced weakening of Asian Summer Monsoon relative to last four centuries, *Geophys. Res. Lett.*, 46, 5469-5479, 2019.
- Sung, M., Kwon, W., Baek, H., Boo, K., Lim, G., Kug, J.: A possible impact of the North Atlantic Oscillation on the east Asian summer monsoon precipitation, *Geophys. Res. Lett.*, 33, L21713, 2006.
- Tan, L., Shen, C-C., Löwemark, L et al.: Rainfall variations in central Indo-Pacific over the past 2700y, *P Natl Acad Sci USA*, 17201-17206, 2019, 10.1073/pnas.1903167116.
- Trouet, V., Esper, J., Graham, N., Baker, A., Scourse, J., and Frank, D.: Persistent Positive North Atlantic Oscillation Mode Dominated the Medieval Climate Anomaly, *Science*, 324, 78-80, 2009.
- Wang, H.: The weakening of the Asian Monsoon Circulation after the End of 1970's, *Adv. Atmos. Sci.*, 18, 376-386, 2001.
- Wu, Z., Wang, B., Li, J., Jin, F.: An empirical seasonal prediction model of the east Asian summer monsoon using ENSO and NAO, *J. Geophys. Res.*, 114, D181120, 2009.
- Yan, H., Sun, L., Wang, Y., Huang, W., Qiu, S., and Yang, C.: A record of the Southern Oscillation Index for the past 2,000 years from precipitation proxies, *Nat. Geosci.*, 4, 611-614, 2011
- Yu, R., Zhou, T.: Seasonality and Three-Dimensional Structure of Interdecadal Change in the East Asian Monsoon, *J. Climate*, 20, 5344-5355, 2007.
- Zhang, H., Griffiths, M., Chiang, J., Kong, W., Wu, S., Atwood, A., Huang, J., Cheng, H., Ning, Y.,

Xie, S.: East Asian hydroclimate modulated by the position of the westerlies during Termination I, *Science*, 362, 580-583, 2018.

Zhou, T., Gong, D., Li, J., Li, B.: Detecting and understanding the multi-decadal variability of the East Asian Summer Monsoon-Recent progress and state of affairs, *Meteorol. Z.*, 13, 455-467, 2009.

Reviewer #2

Dear Editor Dr. Yin and Anonymous Reviewers:

We really appreciate your time and efforts that you have spent in reading, reviewing and handling our manuscript. Your comments and suggestions have greatly improved our manuscript. Following these insightful comments and suggestions, we have conducted a point-to-point revision as listed below. We have reproduced the reviewers' comments in blue fonts, and our responses in black fonts directly below the comments. We hope that our revised manuscript is now considered to be suitable for publication with your high standard journal.

General comments:

(1) In the introduction, in order to better introduce research background to readers, it is necessary to add some more references. For example, after the sentence of Lines 46-48, Lines 49-51 and Lines 61-63. In addition, some references are not properly used (not the most proper one).

Reply: According to your suggestion, we have added more references in lines 46-48, lines 49-51 and lines 61-63 in the revised manuscript, and deleted some references.

(2) Please add more information about the stalagmite sample. For instance, the sample image can be added in the figure 2, including subsample locations of U-Th dates and if possible stable isotopes as well. Was the whole sample (YX262) or only one portion analyzed in this study? What is the mineral of the sample? The authors only mentioned 'calcite record' in the discussion (Line 241).

Reply: Thank you for your suggestions. We have added a sample image in Figure 2 and marked the sampling locations for U-Th dates in the image in our revised manuscript. The whole sample (YX262) is analyzed in our study, and it is composed of white opaque to brown transparent calcite.

(3) For discussion 4.1, in Lines 153-156, "Thus, the stalagmite d18O signal reflects the regional summer monsoon intensity. . . .", how to understand the term "regional summer monsoon intensity"? In addition, the authors should always point out the timescale when they discuss the significance of the stalagmite d18O proxy. In Lines 146-148, "two most recent studies have reconciled these two contradictory interpretations. . . .", it sounds like that the two studies already resolved the debates of the Chinese stalagmite d18O proxy. There are many papers that have addressed to some extent this issue recently, such as Zhao et al., 2018 and Zhang et al., 2019. Additionally, it appears that the cave d18O was considered to be the 'monsoon intensity' and local precipitation as well at different places, lacking a consistency.

Reply: Many thanks for your detailed comments. Recently published review articles greatly enlighten our understanding on how to interpret the stalagmite $\delta^{18}\text{O}$ records in East Asia (Zhang et al., 2019; Cheng et al., 2019). We have re-organization the related content in the revised manuscript and added those new references.

(4) The small amplitude changes in stalagmite d18O value may have complicated mechanisms behind, such as temperature effect, amount effect, source changes, upper stream rainout, and evaporations etc. If explained solely as local rainfall amount, please provide a comparison to the instrumental record for each cave record or cite related published papers.

Reply: Based on your suggestion, we have made a comparison between our stalagmite $\delta^{18}\text{O}$ record and Meiyu reconstruction from historical documents (Ge et al., 2008). The stalagmite $\delta^{18}\text{O}$ record matches the Meiyu rain well on decadal to centennial timescales. When the stalagmite $\delta^{18}\text{O}$ is lighter, the Meiyu rain weakens, and vice versa. We interpret our Yongxing $\delta^{18}\text{O}$ record as the indicator of the Meiyu rain variation.

(5) In the section 4.2, the authors should compare their record with the stalagmite record from Heshang Cave, which is fairly close to Yongxing Cave. I suggest adding the Heshang $\delta^{18}\text{O}$ record in the figure 3, and have a related discussion in the section. In addition, I strongly encourage the authors to compare the Yongxing record with local historical records or cite related papers, which may provide a validation test on the interpretation of the Yongxing $\delta^{18}\text{O}$ record.

Reply: Many thanks for your suggestion. We have added the Heshang $\delta^{18}\text{O}$ record in Figure 4 of our revised manuscript and included a related discussion about their variations therein. In addition, we have compared our $\delta^{18}\text{O}$ record with instrumental precipitation and Meiyu rain reconstruction. Our record shows a good correlation with the Meiyu reconstruction on decadal to centennial timescales (Ge et al., 2008). No significant correlation is found between the Yongxing $\delta^{18}\text{O}$ record and instrumental precipitation as well as temperature records at the Yichang station (see Fig. 1 below in our response). This relationship was also inferred in a comparison with the Heshang record (He et al., 2009).

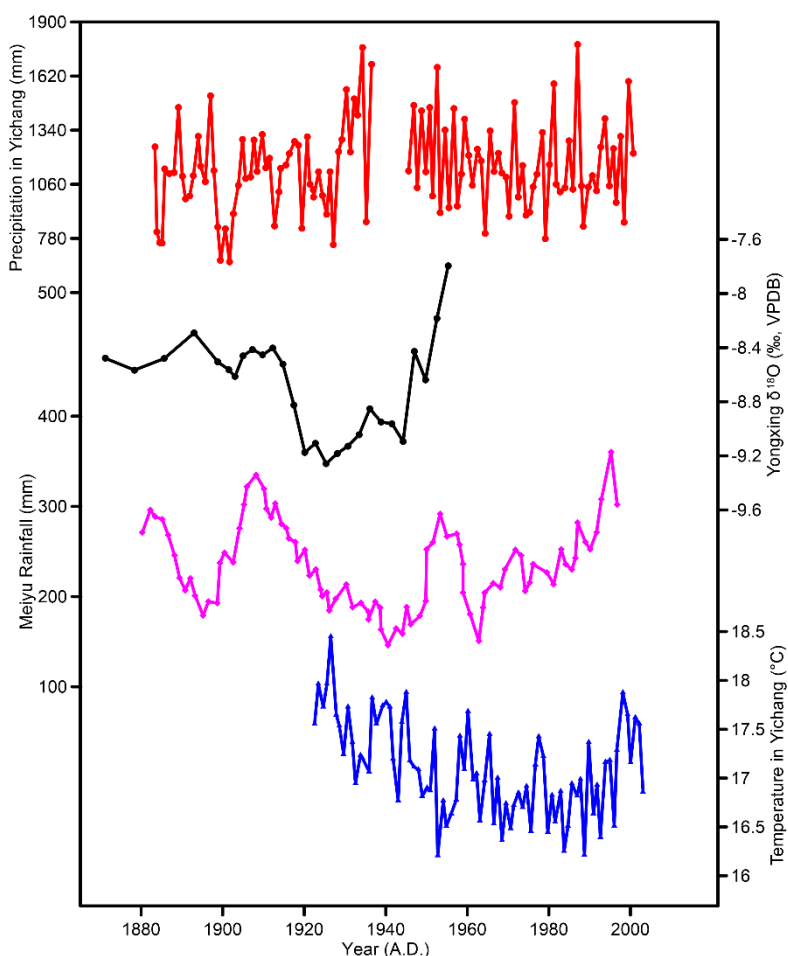


Fig. 1 Comparison of the Yongxing $\delta^{18}\text{O}$ time-series and other records. The black line represents the

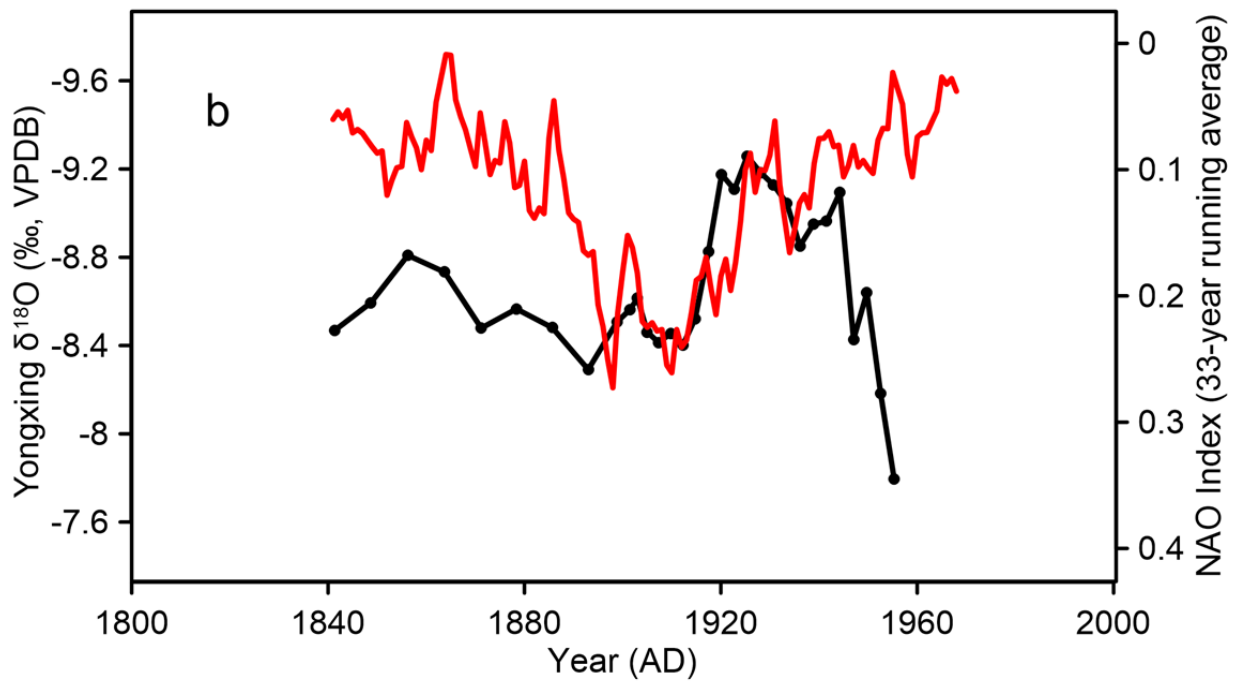
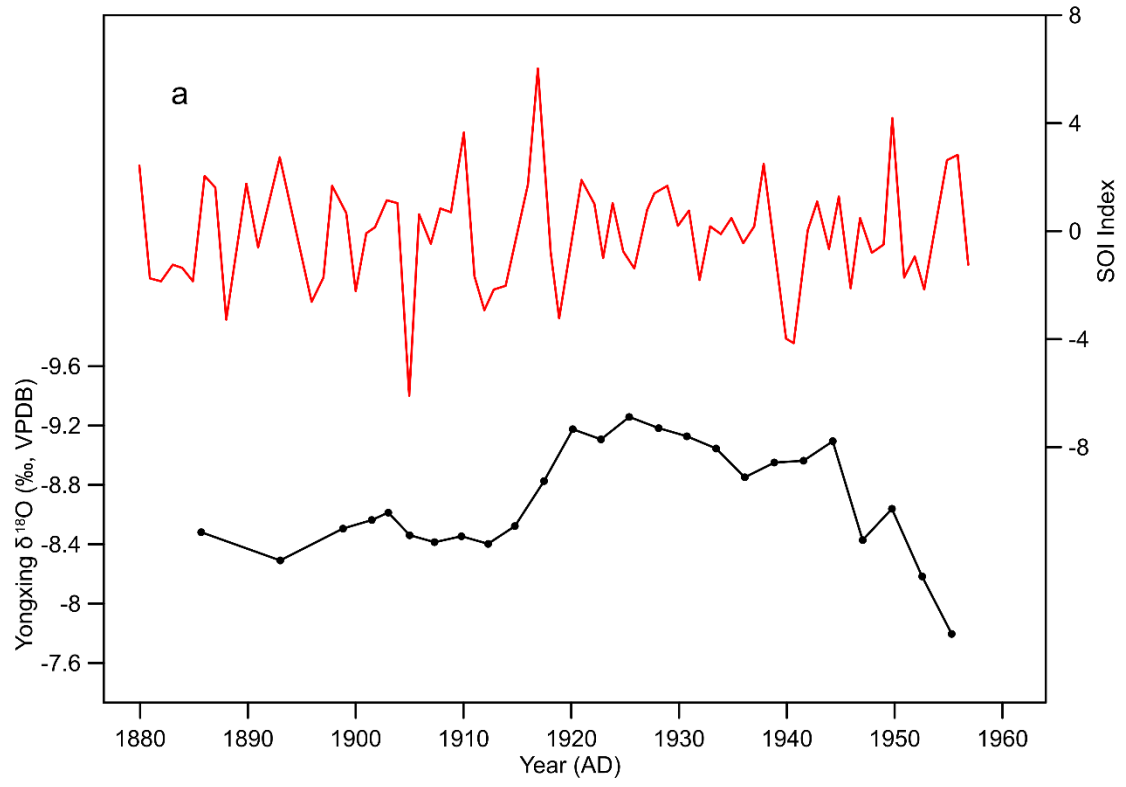
Yongxing $\delta^{18}\text{O}$ time-series; the magenta line indicates Meiyu rain reconstructed from historical documents (Ge et al., 2008); the red and blue lines indicate the instrumental precipitation and temperature at the nearby Yichang station, respectively.

(6) When comparing the $\text{d}18\text{O}$ values between different time periods (the MCA, LIA and CWP), the differences of the mean values should be provided. The trends of records, as well as similarities between different records are merely visually defined. Statistical methods should be considered to show their significances.

Reply: Many thanks for your suggestion. The mean $\delta^{18}\text{O}$ values between the MCA, LIA and CWP represent mean hydrological conditions over these episodes. Our Yongxing $\delta^{18}\text{O}$ record does not cover the whole MCA and CWP episodes. Moreover, the MCA and LIA are not globally coherent (Neukom et al., 2019). Thus, onsets and terminations of these episodes are difficult to unambiguously defined. In our study, we compare $\delta^{18}\text{O}$ minima (drier condition) during the MCA and CWP periods, two warm intervals. The $\delta^{18}\text{O}$ minima could add valuable information to assessing the natural and anthropogenic forcing in central China. The trends of our records have been constrained through the linear fit methods in the revised manuscript. In addition, correlation analyses have been utilized to show significances between two records.

(7) In sections 4.4 and 4.5, I suggest that the authors analyze the relationship of the local precipitation (and/or $\text{d}18\text{O}$) at Yongxing Cave site with ENSO, NAO, PDO and AMOC indexes (reconstructed from instrumental data).

Reply: Following your suggestion, we have made a comparison of the Yongxing $\delta^{18}\text{O}$ record with ENSO, NAO and PDO indexes reconstructed from instrumental data (see Fig. 2 below in our response). No significant correlation is found between them. The AMOC index reconstructed from instrumental data began to exist since 2004, with no temporal overlap with our record. {Since 2004, there has been a major British-American observation project, called RAPID (<http://www.rapid.ac.uk/rapidmoc/overview.php>), which tries to measure the total flow at a particularly suitable latitude (26.5° North) with 226 moored measuring instruments (Meinen et al., 2019).}



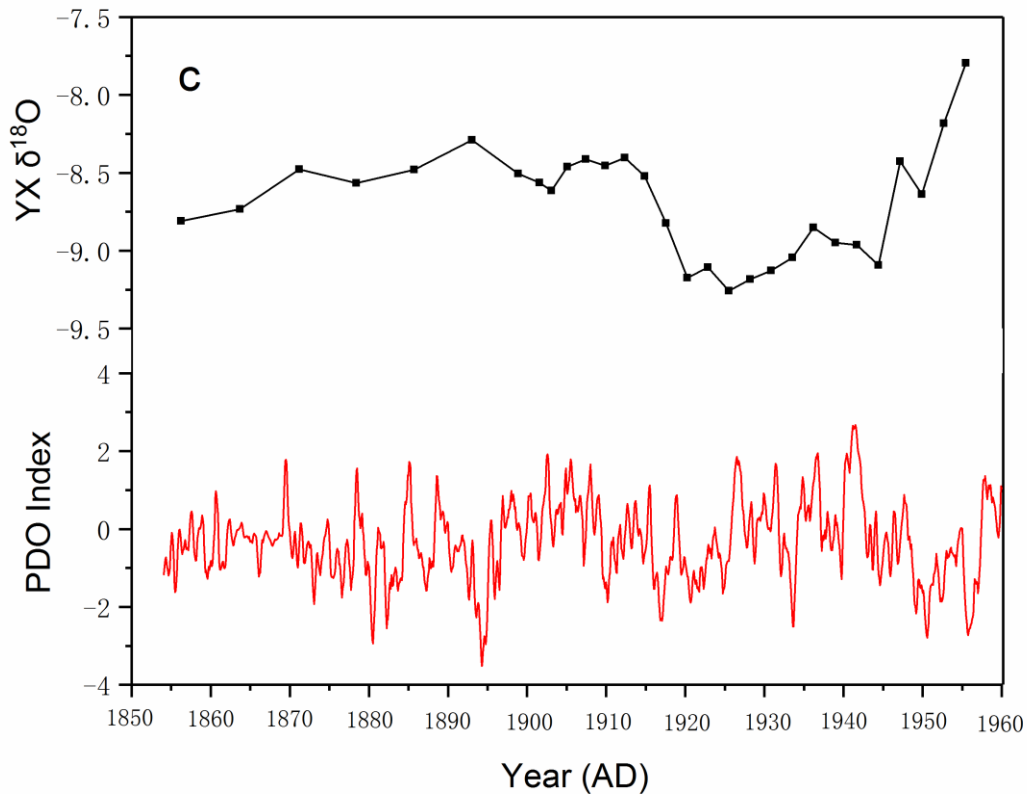


Fig. 2 Comparisons of the Yongxing $\delta^{18}\text{O}$ record and other instrumental data. (a), (b) and (c) show the comparisons of our Yongxing record with SOI, NAO and PDO indexes, respectively. The SOI data is from <http://www.bom.gov.au/climate/current/soihtml.shtml>; the NAO index data is from <https://crudata.uea.ac.uk/cru/data/nao/index.htm>; the PDO index data (Jones et al., 1997) is from <https://www.ncdc.noaa.gov/teleconnections/pdo/>.

(8) Overall, the causal links of the stalagmite $\delta^{18}\text{O}$ records with the AMOC, NAO, ENSO as suggested by the authors are rather tentative. For example, a visual similarity between two records cannot be used to definitively validate their causal linkage.

Reply: Thanks for your suggestion. Based on the Yongxing $\delta^{18}\text{O}$ record, we discuss a potential influence of the Pacific and North Atlantic Oceans on the Meiyu rain. The causal linkage would be examined by future geological records and climate simulations. Regrettably, climate simulation is beyond the scope of our current study. Nevertheless, correlation analyses have been calculated to validate causal linkages in the revised manuscript.

Specific comments:

1. Lines 24-26: I don't think we can say the "EASM intensity is similar in both northern and central China,". I mean we cannot say local EASM intensity instead of local precipitation amount. In addition, the timescale should be always mentioned.

Reply: Thanks very much for your guidance. Following the guidance, we have revised the inaccurate description in lines 24-26 in the reorganized manuscript.

2. Lines 31 and 278: The authors use "surprisingly" twice in the manuscript. Actually, many studies

already found the North Atlantic climate can influence the EASM changes, for example He et al. (2017).

Reply: Thanks for your suggestion. The word of “surprisingly” is inaccurate in lines 31 and 278. Therefore, we have deleted the word in our revised manuscript.

3. Lines 74-77: Zhang et al. (2018), which discussed the EASM precipitation changes in the monsoonal China during the weakening AMOC, may be cited here.

Reply: Thanks for pointing out this important research. We have referred to Zhang et al., (2018) in our revised manuscript.

4. Line 129: The sentence “Stalagmite YX262 was deposited under the condition of isotope equilibrium” should be moved to the end of line 133 as a conclusion.

Reply: Many thanks. The sentence has been moved to the end of line 133 as a conclusion.

5. For the figure 1, what does the background color in the map indicate? If it's meaningful, please add a legend.

Reply: Thanks for your advice, we have modified the figure and added a legend.

References

- Cheng, H., Zhang, H., Zhao, J., Li, H., Ning, Y., Kathayat, G.: Chinese stalagmite paleoclimate researches: A review and perspective, *Sci. China Earth Sci.*, 62, 1489-1513, 2019.
- Ge, Q., Guo, X., Zheng, J., Hao, Z.: Meiyu in the middle and lower reaches of the Yangtze River since 1736, *Chinese Sci. Bull.*, 53, 107-114, 2008.
- He, L., Hu, C., Huang, J., Xie, S., Wang, Y.: Characteristics of large-scale circulation of East Asian Monsoon indicated by oxygen isotope of stalagmite, *Quaternary Science*, 29, 950-956, 2009 (in Chinese with English abstract).
- Jones, P., Jonsson, T., Wheeler, D.: Extension to the North Atlantic oscillation using early instrumental pressure observations from Gibraltar and south-west Iceland, *Int. J. Climatol.*, 17, 1433-1450, 1997.
- Meinen, C., Johns, W., Moat, B., Smith, R. Johns, E., Rayner, D., Frajka-Williams, E., Garcia, R., Garzoli, S.: Structure and Variability of the Antilles Current at 26.5°N, *Journal of Geophysical Research*, <https://doi.org/10.1029/2018JC014836>, 2019.
- Neukom, R., Steiger, N., Gómez-Navarro, J., Wang, J., Werner, J.: No evidence for globally coherent warm and cold periods over the preindustrial Common Era, *Nature*, 571, 550-554, 2019.
- Zhang, H., Brahim, Y., Li, H., Zhao, J., Kathayat, G., Tian, Y., Baker, J., Wang, J., Zhang, F., Ning, Y., Edwards, R., Cheng, H.: The Asian Summer Monsoon: Teleconnections and Forcing Mechanisms-A Review from Chinese Speleothem $\delta^{18}\text{O}$ Records, *Quaternary*, 2, 26, 2019.
- Zhang, H., Cheng, H., Cai, Y., Spötl, C., Kathayat, G., Sinha, A., Edwards, R. L., and Tan, L.: Hydroclimatic variations in southeastern China during the 4.2 ka event reflected by stalagmite records, *Climate of the Past*, 14, 1805-1817, 2018.

1 **Hydrological variations in central China over the past millennium**
2 **and their links to the Tropic Pacific and North Atlantic Oceans**

3 Fucai Duan^{a,*}, Zhenqiu Zhang^{b,c,*}, Yi Wang^{d,e,*}, Jianshun Chen^a, Zebo Liao^c, Shitao
4 Chen^c, Qingfeng Shao^c, Kan Zhao^c

5 ^aCollege of Geography and Environmental Sciences, Zhejiang Normal University,
6 Jinhua 321004, China

7 ^bSchool of Life Sciences, Nanjing Normal University, Nanjing 210023, China

8 ^cCollege of Geography Science, Nanjing Normal University, Nanjing 210023, China

9 ^dDepartment of Geography and School of Global Studies, University of Sussex, Falmer,
10 Brighton BN1 9QJ, UK

11 ^eDepartment of Earth System Science, Institute for Global Change Studies, Tsinghua
12 University, Beijing 100084, China

13 *Corresponding authors:

14 E-mail addresses: fcdan@foxmail.com (F. Duan), zhangzhenqiu163@163.com (Z.
15 Zhang), yi.wang@sussex.ac.uk (Y. Wang)

16 **Abstract:** Variations of precipitation, aka the Meiyu rain, in East Asian summer
17 monsoon (EASM) domain during the last millennium could help enlighten the
18 hydrological response to future global warming. Here we present a precisely dated and
19 highly resolved stalagmite $\delta^{18}\text{O}$ record from the Yongxing Cave, central China. Our
20 new record, combined with a previously published one from the same cave, indicates
21 that the Meiyu rain has changed dramatically in association with the global temperature
22 change. In particular, our record shows that the Meiyu rain has weakened during the
23 Medieval Climate Anomaly (MCA) and the Current Warm Period (CWP), but
24 intensified during the Little Ice Age (LIA). We find that the Meiyu rain is similarly
25 wetter during the MCA and CWP in northern China and similarly drier in central China,
26 but relatively wetter during the CWP in southern China. This discrepancy indicates a
27 complicated localized response of the regional precipitation to the anthropogenic
28 forcing. The weakened (intensified) Meiyu rain during the MCA (LIA) matches well
29 with the warm (cold) phases of Northern Hemisphere surface air temperature. This
30 Meiyu rain pattern also corresponds well with the climatic conditions over the Tropical
31 Indo-Pacific warm pool. On the other hand, our record shows a strong association with
32 the North Atlantic climate as well. The reduced (increased) Meiyu rain correlates well
33 with positive (negative) phases of North Atlantic Oscillation. In addition, our record
34 links well with the strong (weak) Atlantic meridional overturning circulation during the
35 MCA (LIA) period. All above-mentioned localized correspondences and remote
36 teleconnections on decadal to centennial timescales indicate that the Meiyu rain is
37 coupled closely with oceanic processes in the Tropical Pacific and North Atlantic
38 Oceans during the MCA and LIA.

39 **Keywords:** Stalagmite; East Asian summer monsoon; Global warming; Last

40 Millennium; Little Ice Age; Medieval Climate Anomaly; the Meiyu rain

41 **1 Introduction**

42 The last millennium was climatically characterized by the Medieval Climate
43 Anomaly (MCA; 900-1400 AD) and the Little Ice Age (LIA; 1400-1850 AD), and the
44 Current Warm Period (CWP; 1850AD to present). These three episodes attract broad
45 attention within the scientific and policy-making communities, because they contain
46 critical information to distinguish between the natural and anthropogenic climate
47 variability. Origins of the MCA and LIA are attributed to the radiative forcing
48 associated with solar activities and volcanic eruptions, yet the CWP is considered as a
49 result of increasing anthropogenic greenhouse gases (Bradley and Jonest., 1993; Hegerl
50 et al., 2007; Lamouereus et al., 2001; Sigl et al., 2014). In particular, the CWP is much
51 warmer than the MCA (PAGES 2k Consortium, 2013). In association with the global
52 temperature change, East Asian summer monsoon (EASM) precipitation has changed
53 significantly (Paulsen et al., 2003; Zhang et al., 2008; Tan et al., 2009, 2011a, 2015).
54 Many studies have indicated that monsoonal climate of China has generally recorded
55 wetter MCA and drier LIA in the north, but show reverse conditions in the south (Tan
56 et al., 2009, 2018; Chen et al., 2015). However, it is unclear about the hydrological
57 variation during the MCA and LIA over central China. Moreover, less is known about
58 the relative intensity of precipitation between the CWP and MCA, two recent warm
59 periods. The examination of the relative precipitation intensity is the key to evaluating
60 the hydrological responses under the anthropogenic warming.

61 To better understand hydrological responses to the anthropogenic warming, it is
62 necessary to appreciate the natural forcing of the hydrological cycle during the MCA
63 and LIA periods before the greenhouse gas emission. The hydroclimate in the EASM
64 domain is strongly influenced by the Tropical Pacific and North Atlantic Oceans (Wang
65 et al., 2005; Zhang et al., 2018a, Cheung et al., 2018). The Tropical Pacific Ocean feeds
66 the warm and moisture air directly into the EASM domain, and therefore exerts a strong
67 influence (Karami et al., 2015). Several studies have indicated that the hydrological
68 condition in the EASM domain is affected by alternations of La Nina-like and El Nino-
69 like conditions in the Tropical Pacific during the last millennium (e.g., Chen et al., 2015;
70 Zhao et al., 2016; Zhang et al., 2018a). However, these studies did not reach an
71 agreement on how the Tropical Pacific affects hydrological change in the EASM

72 domain. To precisely understand a spatio-temporal evolution of the hydrological cycle,
73 we need to know exactly which changes in the hydrological cycle are linked to which
74 modes of the Pacific atmosphere-ocean circulation during the MCA and LIA in central
75 China. On the other hand, the North Atlantic signal can be transmitted to other parts of
76 the world through the Atlantic meridional overturning circulation (AMOC; Bond et al.,
77 2001). Marine sedimentary records have suggested that strong (weak) AMOC over the
78 warm Greenland interstadials (stadials) correlated tightly with intervals of enhanced
79 (reduced) EASM during the last glaciation (Wang et al., 2001a; Jiang et al., 2016).
80 Similarly, weak EASM episodes occurred in association with ice-rafted events in the
81 North Atlantic, which is capable of weakening the AMOC during the Holocene (Wang
82 et al., 2005; Zhao et al., 2016; Zhang et al., 2018b). This covariation implies a persistent
83 influence of the AMOC on EASM. However, available empirical data is still rare to
84 explore the potential link between the AMOC and regional precipitation (e.g., EASM)
85 during the MCA and LIA intervals.

86 Here we present a new precisely-dated and highly-resolved stalagmite record from
87 Yongxing Cave, Central China. This record, together with a recently published records
88 from the same cave (Zhang W et al., 2019), advances our understanding of the
89 hydrological cycle in East Asia during the last millennium.

90 **2 Materials and methods**

91 Two stalagmites (YX262 and YX275) are used in this study, both from Yongxing
92 Cave (31°35'N, 111°14'E; elevation 800 m above msl; Fig. 1), central China. The
93 previously published stalagmites YX275 has reported detailed variability in the EASM
94 since the LIA (Zhang W et al., 2019). The new candle-like stalagmite YX262 is 159
95 mm long and 55 mm wide. It is composed of white opaque to brown transparent calcite
96 (see Fig. 2). The Yongxing Cave is located between the Chinese Loess Plateau and the
97 Yangtze River. Average annual rainfall is about 1000 mm at the site of the cave.
98 Atmospheric temperature is about 14.3°C and relative humidity is close to 100% inside
99 the cave. The cave site is climatically influenced by East Asian Monsoon, featured with
100 wet and warm summer, and dry and cold winter.

101 Stalagmite YX262 was first halved and then polished for the purpose of the
102 subsequent sampling. For stable isotope analyses, powdered subsamples, weighing
103 about 50-100 µg, were drilled on the polished surface along the central growth axis of

104 the stalagmite. A total of 159 subsamples were obtained at 1 mm increments. The $\delta^{18}\text{O}$
105 measurements were performed on a Finnigan-MAT-253 mass spectrometer at Nanjing
106 Normal University. Results are reported as per mil (‰) against the standard Vienna Pee
107 Dee Belemnite (VPDB). Precision of $\delta^{18}\text{O}$ is 0.06‰ at the 1-sigma level. For U-Th
108 dates, six powdered subsamples, about 100 mg each, were drilled along the central
109 growth layer. Procedures for chemical separation and purification of uranium and
110 thorium were described in Shao et al. (2017). U and Th isotope measurements were
111 performed on a Neptune MC-ICP-MS at Nanjing Normal University. All the dates are
112 in stratigraphic order with uncertainty of less than 3% of the actual dates (see Table 1).

113 **3 Results**

114 **3.1 Chronology**

115 The six U-Th dates and corresponding isotopic ratios are shown in Table 1.
116 Adequate uranium concentrations (0.5–0.7 ppm) and low initial thorium contents (200–
117 700 ppt, with the exception of 1440 ppt) produced precise dates with small age
118 uncertainty (6–20 years). The chronology for the stalagmite was established by the
119 StalAge algorithm (Scholz and Hoffmann, 2011). The age model shows that the
120 stalagmite YX262 was deposited from 1027 to 1639 AD (see Fig. 2). The age-depth
121 plot indicates the growth rate of the stalagmite is stable, reaching 0.26 mm/year. The
122 high and stable growth rate suggests that the stalagmite grew continuously without a
123 significant hiatus. Visual inspections consolidate the continuity of the stalagmite growth.
124 The temporal resolution is 3.8 year, allowing for detailed characterizing the Asian
125 hydroclimate for the first half of the second millennium.

126 **3.2 Stable isotope**

127 The $\delta^{18}\text{O}$ record of YX262 displays a pronounced fluctuation during the whole
128 period (see Fig. 4). The $\delta^{18}\text{O}$ values ranges from -9.31‰ to -7.88‰, averaging -8.60‰.
129 The $\delta^{18}\text{O}$ values decrease gradually from 1027 to 1372 AD, and then increase gradually
130 before rapidly increasing to the ^{18}O -enriched conditions from 1515 AD. The interval
131 with high $\delta^{18}\text{O}$ values is ~100-year long, which is terminated by a pulse to more
132 negative values at 1626 AD. In general, the ^{18}O -depleted interval is coeval with the
133 MCA and the ^{18}O -enriched interval corresponds to the early LIA (see Fig. 4).

134 **4 Discussion**

135 **4.1 The interpretation of our $\delta^{18}\text{O}$**

136 Stalagmite YX262 was deposited under the condition of isotope equilibrium.
137 Relative to the Hendy tests, replication tests have been considered as a more vigorous
138 method to examine the isotope equilibrium (Dorale and Liu, 2009). The YX262 $\delta^{18}\text{O}$
139 record matches another Yongxing cave record during the overlapping interval (see Fig.
140 5; Zhang W et al., 2019), indicating an equilibrium condition for the isotope. A minor
141 difference exists between the two stalagmite $\delta^{18}\text{O}$ records. The YX262 record shows a
142 larger shift toward more negative values than the YX275 record in the early 1600s.
143 Different feeding systems for both the stalagmites probably produce the $\delta^{18}\text{O}$
144 discrepancy. Longer mixing of meteorological rain within the overlying bedrock may
145 dampen the overall rain $\delta^{18}\text{O}$ amplitude and therefore lead to the calcite $\delta^{18}\text{O}$ offsets
146 (Tan et al., 2019; Carolin et al., 2013). The more negative $\delta^{18}\text{O}$ shift occurred at the
147 beginning of the growth of stalagmite YX262. At the beginning, the mixing of
148 meteorological rain within the overlying bedrock is low, resulting to the lighter $\delta^{18}\text{O}$
149 values. Overall, the good replication between the two records suggests that the YX262
150 $\delta^{18}\text{O}$ signal is less influenced by the kinetic fractionation and is primarily of climatic
151 origin. Nevertheless, the climatic significance of the cave $\delta^{18}\text{O}$ record in eastern China
152 remains a long-term scientific debate. For example, the $\delta^{18}\text{O}$ records were considered
153 to reflect changes in moisture sources (so-called “circulation effect”, Tan., 2014, 2016),
154 moisture pathways (Baker et al., 2015), and a combination of the EASM and winter
155 temperature (Clemens et al., 2010, 2018). Two recent review articles have greatly
156 enlightened our understanding of the stalagmite $\delta^{18}\text{O}$ records in the EASM domain
157 (Zhang H et al., 2019; Cheng et al., 2019). They have proposed that the cave $\delta^{18}\text{O}$
158 records have reflected large-scale and integrated changes in the Asian summer monsoon
159 intensity on the orbital and millennial scales. This interpretation is supported by strong
160 correlations among the cave $\delta^{18}\text{O}$ records across China (e.g., Yuan et al., 2004; Zhao et
161 al., 2010; Cheng et al., 2009; 2016) and correlations with climate conditions in major
162 global climate systems, such as Antarctica, Greenland and Westerly climate (see Figs.
163 2 and 3 in Cheng et al., 2019). The lighter stalagmite $\delta^{18}\text{O}$ values signify larger rainout
164 along the moisture trajectory and thus stronger EASM intensity and vice versa.
165 However, the interpretation of the stalagmite $\delta^{18}\text{O}$ records remains complex on the
166 annual to centennial scales, due to a wide range of potential influencing factors, such

167 as summer rainfall, moisture sources and seasonality of precipitation (Zhang H et al.,
168 2019; Cheng et al., 2019). At the Dongge cave location, stalagmite $\delta^{18}\text{O}$ records were
169 interpreted to be associated with the monsoon precipitation on the decadal to centennial
170 scale, because of its covariation with the local hydrological proxy, annual band
171 thickness (Zhao et al, 2015). Our Yongxing $\delta^{18}\text{O}$ record in central China correlates well
172 with Meiyu rain fluctuations in the middle and lower reaches of the Yangtze River on
173 the decadal to centennial scale (see Fig. 3; Ge et al., 2008). When the stalagmite $\delta^{18}\text{O}$
174 values are lighter, the Meiyu rain is lower and vice versa. This relationship is further
175 supported by inverse correlations of stalagmite $\delta^{18}\text{O}$ records with local rainfall variation
176 (trace element ratio and $\delta^{13}\text{C}$) in the nearby Haozhu Cave (Zhang et al., 2018c). As
177 suggested in Zhang et al. (2018c) and Cheng et al. (2019), increased (weakened) EASM
178 would lead to a shorter (longer) Meiyu rain stage and thus a decrease (increase) of
179 precipitation in the middle and lower reaches of the Yangtze River. Thus, the Yongxing
180 $\delta^{18}\text{O}$ signal mainly reflects Meiyu rain conditions on the decadal to centennial scales,
181 with lower and higher $\delta^{18}\text{O}$ values reflecting decreased and increased rainfall,
182 respectively.

183 **4.2 The regional characters of the MCA and LIA**

184 The climate condition during the MCA and LIA has been extensively studied for
185 the monsoonal China (e.g., Chen et al., 2015; Xu et al., 2016; Tan et al., 2018). In
186 general, wetter in the north and drier in the south were inferred during the MCA and
187 the opposite during the LIA (e.g., Chen et al., 2015; Tan et al., 2018). The boundary
188 between the north and south of China was estimated to be about along the River Huai
189 at 34°N (Chen et al., 2015), the modern geographical dividing line between northern
190 and southern China. As an interesting exception, the Dongge cave records in Guizhou,
191 Southwestern China ($25^\circ17'\text{N}$, $108^\circ5'\text{E}$) showed a wetter MCA and drier LIA (see Fig.
192 4; Wang et al., 2005; Zhao et al., 2015). This is consistent with strong spatiotemporal
193 variability of precipitation in the broad EASM region.

194 Our Yongxing record, slightly south to 34°N , is further supported by the nearby
195 Heshang $\delta^{18}\text{O}$ record, despite larger chronological offsets between them (see Fig. 4; Hu
196 et al., 2008). Both stalagmite $\delta^{18}\text{O}$ records consistently show a trend toward lighter
197 values over the MCA period and a double valley structure over the LIA period. An extra
198 comparison shows that the Yongxing and Heshang (Hu et al., 2008) $\delta^{18}\text{O}$ records in
199 central China vary broadly in phase with the Dongge record in the south, as well as

200 Wanxiang (Zhang et al., 2008) and Huangye (Tan et al., 2011b) records in the north.
201 These cave records indicate a drier MCA and wetter LIA in central China, but the
202 opposite in the north and south (see Fig. 4). Again, a minor but important discrepancy
203 exists between these cave records during the MCA. The cave records in the south
204 display an increasing precipitation trend, but those in the northern and central China
205 reflect a decreasing trend during the MCA (see Fig. 4 for the trends indicated by the
206 arrows). To explain this discrepancy, we compare all the cave records to changes in
207 temperatures of Northern Hemisphere (Mann et al., 2009) and northern China (Tan et
208 al., 2003), and meridional displacement of the Intertropical Convergence Zone (ITCZ;
209 Haug et al., 2001). The result indicates that all the cave records collectively exhibit a
210 broad similarity to the variation in the temperatures and the displacement of the ITCZ
211 (see Fig. 4). Detailed inspection displays that the weakening precipitation signal
212 recorded in the northern caves during the MCA is linked with the decreasing
213 temperatures in the Northern Hemisphere and northern China. In contrast, the
214 intensifying signal recorded in the southern cave during the MCA corresponds to the
215 northward displacement of the ITCZ. The comparison indicates that the different
216 climate patterns between the south and north may result from different controlling
217 factors at lower and higher latitudes, respectively. The ‘north drought’ and ‘south flood’
218 can result from meridional migration of the Meiyu rain belt (Yu and Zhou., 2007; Zhou
219 et al., 2009; Zhang et al., 2018c). It seems that the cold temperature from the north
220 restrains the northward migration of the Meiyu rain belt related to the movement of the
221 ITCZ during the MCA, leading to the hydrological seesaw between the northern and
222 central China. It is noted that the enhanced precipitation condition documented in the
223 Dongge records is contradictory with those reported in many other paleoclimate records
224 in the south. For example, drier MCA and wetter LIA were suggested in an integrated
225 stalagmite $\delta^{18}\text{O}$ record from Sichuan Province (Tan et al., 2018), a pollen-derived
226 rainfall record near the Yongxing Cave site (He et al., 2003), and a lake-based rainfall
227 record in Guangdong Province (Chu et al., 2002). This regional discrepancy can be
228 checked by additional highly-resolved and precisely dated records in southern China.

229 **4.3 The hydrological condition during the MCA as compared to the CWP**

230 A comparison of the relative intensity of precipitation between the MCA and CWP
231 could be useful to evaluate the hydrological response towards the current global
232 warming. Many studies have found that the CWP is much warmer than the MCA on

233 global and hemispheric scales (Bradley et al., 2003; Mann et al., 2008, 2009; PAGES
234 2k Consortium, 2013). With regard to the hydrological response, northern China shows
235 an increased or comparable precipitation maximum during the MCA as compared to
236 the CWP (e.g., the Wanxiang and Huangye Caves' records in Fig. 4). A similar
237 precipitation minimum is documented in the Yongxing and Heshang records in central
238 China (see Fig. 4). However, two Dongge records in southern China collectively shows
239 a slight decrease in precipitation maximum during the MCA as compared to the CWP
240 (see Figs. 4, 5). This is indicated by a 0.39‰ higher $\delta^{18}\text{O}$ maximum during the MCA
241 than the CWP (see Fig. 5). The increased precipitation during the CWP relative to the
242 MCA is parallel to the global temperature evolution, in particular in the western Pacific
243 Warm Pool region (Chen et al., 2018). This correspondence supports the hypothesis that
244 current global warming intensifies the Asian summer monsoon (Wang et al., 2013). The
245 intensified Asian summer monsoon was suggested due to strong coupling of the climate
246 system related to the global warming. Wang et al. (2013) have stated a mega ENSO
247 condition could trigger a stronger EASM in the CWP through the intensified Hadley
248 and Walker circulations. On the other hand, southern China is partially influenced by
249 the Indian Ocean, which also brings moisture to the area of our study (An et al., 2011).
250 We suggest the small discrepancy between Yongxing and Dongge records could be due
251 to the different localized effects in southern China as Dongge Cave is much closer to
252 Indian Ocean than Yongxing Cave.

253 Different scenarios exist in the South China Sea regarding to the hydrologic
254 variation between the MCA and CWP. The South China Sea is climatically influenced
255 by the EASM and tropical Pacific climate. The lacustrine and coralline records
256 collectively indicate a comparative climate condition between the MCA and CWP (e.g.,
257 Yan et al., 2011b; Deng et al., 2017). The MCA and CWP are considered to be drier
258 than the LIA in the South China Sea. Yan et al. (2011b) highlighted that a decrease and
259 eastward shift of the Pacific Walker circulation were responsible primarily for the drier
260 climate condition during the MCA and CWP. However, changes in the Walker
261 circulation (Yan et al., 2011b) are in contrast to other estimations (Wang et al., 2013;
262 Cobb et al., 2003), which suggested a strong and westward Pacific Walker circulation
263 during the warm periods. Due to the contradiction on the Pacific Walker circulation
264 changes, the trigger for the intensified Asian monsoon during the CWP needs further
265 verification. Therefore, continued studies are needed on the links between the EASM
266 and the Pacific climate.

267 **4.4 The link to the equatorial Tropical Pacific Ocean**

268 The ITCZ and El Niño-Southern Oscillation (ENSO) exert profound influences on
269 the precipitation in East Asia during the last millennium (Wang et al., 2013). As shown
270 in Fig. 6, our calcite record shows a great similarity to temperature and hydrology
271 reconstructions over the Tropical Indo-Pacific warm pool (IPWP). High-resolution
272 sediment (Oppo et al., 2009) and speleothem (Griffiths et al., 2016) records over the
273 IPWP collectively suggest warm sea surface temperatures and increased rainfall during
274 the MCA and CWP, and reversed conditions during the LIA (Fig. 6). The rainfall over
275 the IPWP is linked with the Meiyu rain. This correlation probably stems from
276 modulations of the ITCZ' latitudinal migration on the EASM during the last millennium
277 (Zhao et al., 2015; Xu et al., 2016; Griffiths et al., 2016). In addition, the temperature
278 change over the IPWP can indirectly influence the Meiyu rain via the expansion and
279 contraction of the ITCZ (Yan et al., 2015; Chen et al., 2018). The warm MCA and cold
280 LIA conditions do not necessarily signify a La Nina-like condition during the MCA and
281 an El Nino-like condition during the LIA over the IPWP. Conversely, rainfall-based
282 ENSO reconstructions showed the El Nino- and La Nina-like conditions during the
283 MCA and LIA, respectively (Moy et al., 2002, Yan et al., 2011a; Fig. 6e, f). The
284 sediment-derived ENSO variation in Ecuador (Moy et al., 2002) and the composite
285 ENSO reconstruction across the Tropic Pacific (Yan et al., 2011a) showed a great
286 similarity among the ENSO signals and the timing of switches between the ENSO cold
287 and warm phases. These ENSO reconstructions resemble well with Yongxing records
288 (see Fig. 6; $R_{YX \text{ record-composite ENSO}}=0.18$, $P<0.05$, $N=186$). For example, the El Nino- and
289 La Nina-like conditions during the MCA and LIA parallel with the decreased and
290 increased Meiyu rain from the Yongxing Cave, respectively. In particular, the switch of
291 the ENSO phases from the MCA to LIA coincides with the Meiyu rain minimum during
292 the MCA (see Fig. 6). These strong correlations indicate a dynamical link between the
293 Meiyu rain and ENSO modes. In the summer after the El Niño evolves to maturity, an
294 abnormally blocked anticyclone takes place in Northeast Asia. At the same time, the
295 subtropical high in the western North Pacific extends westward abnormally. This
296 abnormal circulation pattern strengthens the EASM in subtropical East Asia (Wang et
297 al., 2001b). The strengthened EASM leads to more rain over northern China and less
298 over central China (Zhang et al., 2018c). Despite the potential Meiyu-ENSO link, the
299 ENSO reconstructions still need further verification due to their different variations. A
300 recent temperature record in eastern equatorial Pacific (Rustic et al., 2015) supports the

301 rainfall-based ENSO reconstruction (Moy et al., 2002; Yan et al., 2011a), with the El
302 Nino- and La Nina-like mode during the MCA and LIA, respectively. This record
303 challenges the paradigm of the La Nina-like pattern during the MCA followed by the
304 El Nino-like pattern during the LIA (Cobb et al., 2003). However, the study of Rustic
305 et al. (2015) showed the strongest El Nino-like situation occurred at the late MCA to
306 early LIA transition, instead of the peak MCA.

307 **4.5 The link to the North Atlantic Climate**

308 Our Yongxing record shows a good correlation with the North Atlantic climate. As
309 illustrated in Fig. 7, the decreased (increased) Meiyu rain during the MCA (LIA)
310 coincides with a persistent positive (neutral to slightly negative) North Atlantic
311 Oscillation index (NAO; Trouet et al., 2009; see Fig. 7c; $R=-0.19$; $P<0.05$; $N=182$). In
312 addition, these Meiyu rain variations resemble changes of the Atlantic meridional
313 overturning circulation (AMOC), measured by the drift ice index (see Fig. 7d; Bond et
314 al., 2001) and mean grain size of sortable silt (see Fig. 7e; Thornalley et al., 2018;
315 $R=0.39$; $P<0.01$; $N=186$) in the North Atlantic. The decreased Meiyu rain corresponds
316 to the strong AMOC during the MCA and the increased Meiyu rain to the weak AMOC
317 during the LIA. These strong correlations indicate an influence of the NAO and AMOC
318 on the EASM. During the MCA, positive NAO induces a warmer winter in Europe,
319 which reduces snow accumulation over Eurasia and therefore allows for a farther
320 penetration inland of the EASM next summer (Overpeck et al., 1996). An analysis of
321 instrumental data indicates that the winter NAO signal can be transmitted to East Asia
322 through a wave train bridge and leads to a drier southern China but slightly wetter
323 central China (Sung et al., 2006). On the other hand, Wu et al. (2009) have proposed
324 that NAO-related spring SST anomalies in the North Atlantic can produce anomalous
325 anticyclonic circulations over the Okhotsk Sea, which help to enhance the subtropical
326 monsoon front. Robust AMOC can intensify the EASM through northward positioning
327 the ITCZ (Wang et al., 2017). During the LIA, weaker NAO and AMOC would produce
328 decreased EASM in the reversed fashion. It has been proposed that conditions of the
329 NAO are dynamically coupled to states of the AMOC (Trouet et al., 2009; Wanamaker
330 et al., 2012). The strong (weak) NAO during the MCA (LIA) contributes to enhanced
331 (weakened) AMOC through enhancing (weakening) the westerly (Trouet et al., 2009).
332 On the other hand, solar activity is usually considered as the root trigger of natural
333 climate change. The Yongxing record is broadly similar to changes in solar irradiance

334 (Steinhilber et al., 2009; see Fig. 7a). The decreased Meiyu rain is paralleled with the
335 greater solar activity during the MCA and the increased Meiyu rain with the less solar
336 activity during the LIA. The solar forcing of the Meiyu rain variation, dependent on the
337 EASM strength (Zhang et al., 2018c), can be conducted through modulating the Asia-
338 Pacific temperature contrast (Kutzbach et al., 2008), the AMOC intensity (Wang et al.,
339 2005) and the ENSO condition (e.g., Asmerom et al., 2007; Zhao et al., 2016). However,
340 relative importance of these forcing pathways is unknown and, most importantly, the
341 ENSO condition remains a matter of debate during the last millennium (e.g., Cobb et
342 al., 2003; Yan et al., 2011a). As a counterpart to the MCA, the CWP is similarly marked
343 by decreased Meiyu rain, strong AMOC and high solar output (see Fig. 7). However,
344 the relationship between the Meiyu rain and NAO condition is not significant during
345 the CWP, with the decreased Meiyu rain failing to match the expected more positive
346 NAO. Longer term data from instrumental observations and historical proxies is needed
347 to assess the linkage between NAO condition and Meiyu rain during the CWP.

348 **5 Conclusions**

349 Based on a new and a recently published stalagmite records from the Yongxing
350 cave, central China, we reconstruct a continuous evolutionary history of the Meiyu rain
351 during the past millennium and link its variation with the Pacific and North Atlantic
352 climates. The climatic characters in our record are generally antiphase with those in the
353 Wanxiang and Huangye cave records in northern China. The decreased (increased)
354 Meiyu rain during the MCA (LIA) correlates with the warm (cold) surface temperature
355 and enhanced (reduced) rainfall over the IPWP. Based on the strong correlation with
356 the ENSO reconstruction, our records support an El Nino-like condition during the
357 MCA and a La Nina-like condition during the LIA. In addition, our records show a
358 potential link between the Meiyu rain and the North Atlantic climate. The decreased
359 Meiyu rain coincides with substantially positive NAO and robust AMOC during the
360 MCA, while the increased Meiyu rain corresponds with neutral to negative NAO and
361 weak AMOC during the LIA.

362 **Data availability**

363 Data in this study are available on request.

364 **Competing interests**

365 The authors declare that they have no conflict of interest.

366 **Author contributions**

367 FD, ZZ and YW designed the study and wrote the manuscript. FD, ZZ, YW and
368 JC revised the manuscript. FD, QS, ZL and KZ performed ²³⁰Th dating and oxygen
369 isotope measurements. FD and SC collected samples. All authors discussed the results
370 and contributed to the manuscript.

371 **Acknowledgments**

372 This work was supported by Zhejiang Provincial Natural Science Foundation (no.
373 LY19D020001) and National Natural Science Foundation of China grants (nos.
374 41602181, 41572340 and 41572151). We are grateful to Editor Dr. Qiuzhen Yin and
375 two anonymous reviewers for their helpful suggestions and comments that have greatly
376 improved this manuscript.

377 **References**

- 378 An, Z., Clemens, S., Shen, J., Qiang, X., Jin, Z., Sun, Y., Prell, W., Luo, J., Wang, S., Xu, H.,
379 Cai, Y., Zhou, W., Liu, W., Shi, Z., Yan, L., Xiao, X., Chang, H., Wu, F., Ai, L., and Lu, F.:
380 Glacial-interglacial Indian summer monsoon dynamics, *science*, 333, 719-723, 2011.
- 381 Asmerom, Y., Polyak, V., Burns, S., and Rasmussen, J.: Solar forcing of Holocene climate:
382 New insights from a speleothem record, southwestern United States, *Geology*, 35, 1-4, 2007.
- 383 Baker, A., Sodemann, H., Baldini, J., Breitenbach, S., Johnson, K., Hunen, J., Zhang, P.:
384 Seasonality of westerly moisture transport in the East Asian summer monsoon and its
385 implications for interpreting precipitation $\delta^{18}\text{O}$, *J. Geophys. Res. Atmos.*, 120, 5850-5862,
386 2015.
- 387 Bond, G., Kromer, B., Beer, J., Muscheler, R., Evans, M., Showers, W., Hoffmann, R., Lotti-
388 Bond, R. Hajdas, I., and Bonani, G.: Persistent Solar Influence on North Atlantic Climate
389 During the Holocene, *Science*, 294, 2130-2136, 2001.
- 390 Bradley, R., Hughes, M., and Diaz, H.: Climate in Medieval Time, *Science*, 302, 404-405, 2003.
- 391 Bradley, R., Jonest, P.: 'Little Ice Age' summer temperature variations: their nature and
392 relevance to recent global warming trends, *Holocene*, 3, 367-376, 1993.
- 393 Carolin, S., Cobb, K., Adkins, J., Clark, B., Conroy, J., Lejau, S., Malang, J., Tuen, A.: Varied
394 response of western Pacific hydrology to climate forcings over the last glacial period, *Science*,
395 340, 1564-1566, 2013.
- 396 Chen, J., Chen, F., Feng, S., Huang, W., Liu, J., and Zhou, A.: Hydroclimatic changes in China

397 and surroundings during the Medieval Climate Anomaly and Little Ice Age: spatial patterns
398 and possible mechanisms, *Quaternary Sci. Rev.*, 107, 98-111, 2015.

399 Chen, T., Cobb, K., Roff, G., Zhao, J., Yang, H., Hu, M., and Zhao, K.: Coral-derived western
400 Pacific tropical sea surface temperatures during the last millennium, *Geophys. Res. Lett.*, 45,
401 3542-3549, 2018.

402 Cheng, H., Edwards, R. L., Broecker, W. S., Denton, G. H., Kong, X., Wang, Y., Zhang, R., and
403 Wang, X.: Ice age terminations, *science*, 326, 248-252, 2009.

404 Cheng, H., Edwards, R. L., Sinha, A., Spötl, C., Yi, L., Chen, S., Kelly, M., Kathayat, G., Wang,
405 X., Li, X., Kong, X., Wang, Y., Ning, Y., and Zhang, H.: The Asian monsoon over the past
406 640,000 years and ice age terminations, *Nature*, 534, 640-646, 2016.

407 Cheng, H., Zhang, H., Zhao, J., Li, H., Ning, Y., Kathayat, G.: Chinese stalagmite paleoclimate
408 researches: A review and perspective, *Sci. China Earth Sci.*, 62, 1489-1513, 2019.

409 Cheung, R., Yasuhara, M., Mamo, B., Katsuki, K., Seto, K., Takata, H., Yang, D., Nakanishi,
410 T., Yamada, K., Iwstani, H.: Decadal-to Centennial-Scale East Asian Summer Monsoon
411 variability over the past millennium: An Oceanic Perspective, *Geophys. Res. Lett.*, 45, 7711-
412 7718, 2018.

413 Chu, G., Liu, J., Sun, Q., Lu, H., Gu, Z., Wang, W., and Liu, T.: The 'Mediaeval Warm Period'
414 drought recorded in Lake Huguangyan, tropical South China, Holocene, 12, 511-516, 2002.

415 Clemens, S., Holbourn, A., Kubota, Y., Lee, K., Liu, Z., Chen, G., Nelson, A., Fox-Kemper, B.:
416 Precession-band variance missing from East Asian monsoon runoff, *Nat. Commun.*, 9, 3364,
417 2018.

418 Clemens, S., Prell, W., Sun, Y.: Orbital-scale timing and mechanisms driving Late Pleistocene
419 Indo-Asian summer monsoons: Reinterpreting cave speleothem $\delta^{18}\text{O}$, *Paleoceanography*, 25,
420 PA4207, 2010.

421 Cobb, K., Charles, C., Cheng, H., and Edwards, R.: El Nino/Southern Oscillation and tropical
422 Pacific climate during the last millennium, *Nature*, 424, 271-276, 2003.

423 Deng, W., Liu, X., Chen, X., Wei, G., Zeng, T., Xie, L., and Zhao, J.: A comparison of the
424 climates of the Medieval Climate Anomaly, Little Ice Age, and Current Warm Period
425 reconstructed using coral records from the northern South China Sea, *J. Geophys. Res.-*
426 *Oceans.*, 122, 264-275, 2017.

427 Dorale, J., and Liu, Z.: Limitations of Hندی test criteria in judging the paleoclimate suitability
428 of speleothems and the need for replication, *J. Cave Karst Stud.*, 71,73-80, 2009.

429 Ge, Q., Guo, X., Zheng, J., Hao, Z.: Meiyu in the middle and lower reaches of the Yangtze
430 River since 1736, *Chinese Sci. Bull.*, 53, 107-114, 2008.

431 Griffiths, M., Kimbrough, A, Gagan, M., Drysdale, R., Cole, J., Johnson, K., Zhao, J., Cook,
432 B., Hellstrom, J., and Hantoro, W.: Western Pacific hydroclimate linked to global climate
433 variability over the past two millennia, *Nat. Commun.*, 7, 11719, 2016.

434 Haug, G., Hughen, K., Sigman, D., Peterson, L., and Röhl, U.: Southward migration of the
435 intertropical convergence zone through the Holocene, *Science*, 293, 1304-1308, 2001.

436 He, B., Zhang, S., and Cai, S.: Climatic changes recorded in peat from the Dajiu Lake basin in
437 Shennongjia since the last 2600 years, *Mar. Geol. Quat. Geol.*, 23, 109-115, 2003 (in Chinese
438 with English abstract).

439 Hegerl, G., Crowley, T., Allen, M., Hyde, W., Pollack, H., Smerdon, J., Zorita, E.: Detection of
440 Human Influence on a New, Validated 1500-Year Temperature Reconstruction, *J. Climate*,

441 20, 650-666, 2007.

442 Hu, C., Henderson, G., Huang, J., Xie, S., Sun, Y., Johnson, K.: Quantification of Holocene
443 Asian monsoon rainfall from spatially separated cave records, *Earth Planet Sci. Lett.*, 266,
444 221-232, 2008.

445 Jiang, X., Wang, X., He, Y., Hu, H. M., Li, Z., Spötl, C., and Shen, C. C.: Precisely dated
446 multidecadally resolved Asian summer monsoon dynamics 113.5–86.6 thousand years
447 ago, *Quaternary Sci. Rev.*, 143, 1-12, 2016.

448 Karami, M., Herold, N., Berger, A., Yin, Q., Muri, H.: State of the tropical Pacific Ocean and
449 its enhanced impact on precipitation over East Asia during marine isotopic stage 13, *Clim.
450 Dyn.*, 44, 807-825, 2015.

451 Kutzbach, J., Liu, X., Liu, Z., and Chen, G.: Simulation of the evolutionary response of global
452 summer monsoons to orbital forcing over the past 280,000 years, *Clim. Dynam.*, 2008, 30,
453 567-579, 2008.

454 Lamoureux, S., England, J., Sharp, M., Bush, A.: A varve record of increased ‘Little Ice Age’
455 rainfall associated with volcanic activity, Arctic Archipelago, Canada, *Holocene.*, 11, 243-
456 249, 2001.

457 Mann, M., Zhang, Z., Hughes, M., Bradley, R., Miller, S., Rutherford, S., and Ni, F.: Proxy-
458 Based Reconstructions of Hemispheric and Global Surface Temperature Variations over the
459 Past Two Millennia, *P. Natl. Acad. Sci. USA.*, 105, 13252-13257, 2008.

460 Mann, M., Zhang, Z., Rutherford, S., and Bradley, R., Hughes, M., Shindell, D., Ammann, C.,
461 Faluvegi, G., and Ni, F.: Global Signatures and Dynamical Origins of the Little Ice Age and
462 Medieval Climate Anomaly, *Science*, 326, 1256-1260, 2009.

463 Moy, C., Seltzer, G., Rodbell, D., and Anderson, D.: Variability of El Niño/Southern Oscillation
464 activity at millennial timescales during the Holocene epoch, *Nature*, 420, 162-165, 2002.

465 Oppo, D., Rosenthal, Y., and Linsley, B.: 2,000-year-long temperature and hydrology
466 reconstructions from the Indo-Pacific warm pool, *Nature*, 460, 1113-1116, 2009.

467 Overpeck, J., Anderson, D., Trumbore, S., and Prell, W.: The southwest Indian Monsoon over
468 the last 18000 years, *Clim. Dynam.*, 12:213-225, 1996.

469 PAGES 2k Consortium.: Continental-scale temperature variability during the past two
470 millennia, *Nat. Geosci.*, 6, 339-346, 2013.

471 Paulsen, D., Li, H., Ku, T.: Climate variability in central China over the last 1270 years revealed
472 by high-resolution stalagmite records, 22, 691-701, 2003.

473 Rustic, G., Koutavas, A., Marchitto, T., and Linsley, B.: Dynamical excitation of the tropical
474 Pacific Ocean and ENSO variability by Little Ice Age cooling, *Science*, 350, 1537-1541,
475 2015.

476 Scholz, D., and Hoffmann, D.: StalAge-An algorithm designed for construction of speleothem
477 age models, *Quat. Geochronol.*, 6, 369-382, 2011.

478 Shao, Q., Pons-Branchu, E., Zhu, Q., Wang, W., Valladas, H., and Fontugne, M.: High precision
479 U/Th dating of the rock paintings at Mt. Huashan, Guangxi, southern China, *Quat. Res.*, 88,
480 1-13, 2017.

481 Sigl, M., McConnell, J., Toohey, M., Curran, M., Das, S., Edwards, R., Isaksson, E., Kawamura,
482 K., Kipfstuhl, S., Krüger, K., Layman, L., Maselli, O., Motizuki, Y., Motoyama, H., Pasteris,
483 D., Severi, M.: Insights from Antarctica on volcanic forcing during the Common Era, *Nat.
484 Clim. Change*, 4, 693-697, 2014.

485 Steinhilber, F., Beer, J., and Frohlich, C.: Total solar irradiance during the Holocene, *Geophys.*
486 *Res. Lett.*, 36, L19704, <https://doi.org/10.1029/2009GL040142>, 2009.

487 Sung, M., Kwon, W., Baek, H., Boo, K., Lim, G., Kug, J.: A possible impact of the North
488 Atlantic Oscillation on the east Asian summer monsoon precipitation, *Geophys. Res. Lett.*,
489 33, L21713, 2006.

490 Tan, L., Cai, Y., An, Z., Cheng, H., Shen, C., Breitenbach, S., Gao, Y., Edwards, R., Zhang, H.,
491 Du, Y.: A Chinese cave links climate change, social impacts, and human adaptation over the
492 last 500 years, *Sci. Rep.*, 5, 12284, 2015.

493 Tan, L., Cai, Y., An, Z., Edwards, R., Cheng, H., Shen, C., and Zhang, H.: Centennial-to
494 decadal-scale monsoon precipitation variability in the semi-humid region, northern China
495 during the last 1860 years: Records from stalagmites in Huangye Cave, Holocene, 21, 287-
496 296, 2011b.

497 Tan, L., Cai, Y., An, Z., Yi, L., Zhang, H., Qin, S.: Climate patterns in north central China during
498 the last 1800 yr and their possible driving force, *Clim. Past*, 7, 685-692, 2011a.

499 Tan, L., Cai, Y., Cheng, H., An, Z., and Edwards, R.: Summer monsoon precipitation variations
500 in central China over the past 750 years derived from a high-resolution absolute-dated
501 stalagmite, *Palaeogeogr. Palaeoclimatol.*, 280, 432-439, 2009.

502 Tan, L., Cai, Y., Cheng, H., Edwards, L., Lan J., Zhang, H., Li, D., Ma, L., Zhao, P., and Gao,
503 Y.: High resolution monsoon precipitation changes on southeastern Tibetan Plateau over the
504 past 2300 years, *Quaternary Sci. Rev.*, 195, 122-132, 2018.

505 Tan, L., Shen, C., Löwemark, L., Chawchai, S., Edwards, R., Cai, Y., Breitenbach, S., Cheng,
506 H., Chou, Y., Duerrast, H., Partin, J., Cai, W., Chabangborn, A., Gao, Y., Kwecien, O., Wu,
507 C., Shi, Z., Hsu, H., Wohlfarth, B.: Rainfall variations in central Indo-Pacific over the past
508 2700 y, *P. Natl. Acad. Sci. USA.*, 17201-17206, [10.1073/pnas.1903167116](https://doi.org/10.1073/pnas.1903167116), 2019.

509 Tan, M., Liu, D., Hou, J., Qin, X., Zhang, H., and Li, T.: Cyclic rapid warming on centennial-
510 scale revealed by a 2650-year stalagmite record of warm season temperature, *Geophys. Res.*
511 *Lett.*, 30, 1617, <https://doi.org/10.1029/2003GL017352>, 2003.

512 Tan, M.: Circulation background of climate patterns in the past millennium: Uncertainty
513 analysis and re-reconstruction of ENSO-like state, *Sci. China Earth Sci.*, 59, 1255-1241,
514 <https://doi.org/10.1007/s11430-015-5256-6>, 2016.

515 Tan, M.: Circulation effect: response of precipitation $\delta^{18}\text{O}$ to the ENSO cycle in monsoon
516 regions of China, *Clim. Dyn.*, 42, 1067-1077, 2014.

517 Thornalley, D., Oppo, D., Ortega, P., Robson, J., Brierley, C., Davis, R., Hall, I., Moffa-Sanchez,
518 P., Rose, N., Spooner, P., Yashayaev, I., and Keigwin, L.: Anomalously weak Labrador Sea
519 convection and Atlantic overturning during the past 150 years, *Nature*, 556, 227-230, 2018.

520 Trouet, V., Esper, J., Graham, N., Baker, A., Scourse, J., and Frank, D.: Persistent Positive North
521 Atlantic Oscillation Mode Dominated the Medieval Climate Anomaly, *Science*, 324, 78-80,
522 2009.

523 Wanamaker Jr, A., Butler, P., Scourse, J., Heinemeier, J., Eiriksson, J., Knudsen, K., and
524 Richardson, C.: Surface changes in the North Atlantic meridional overturning circulation
525 during the last millennium, *Nat. Commun.*, 3, 899, 2012.

526 Wang, B., Liu, J., Kim, H., Webster, P., Yim, S. and Xiang, B.: Northern Hemisphere summer
527 monsoon intensified by mega-El Nino/southern oscillation and Atlantic multidecadal
528 oscillation, *P. Natl. Acad. Sci. USA.*, 110, 5347-5352, 2013.

529 Wang, X., Edwards, R., Auler, A., Cheng, H., Kong, X., Wang, Y., Cruz, F., Dorale, J., and
530 Chiang, H.: Hydroclimate changes across the Amazon lowlands over the past 45,000 years,
531 *Nature*, 541, 204-207, 2017.

532 Wang, Y., Cheng, H., Edwards, R., An, Z., Wu, J., Shen, C., and Dorale, J.: A high-resolution
533 absolute-dated late Pleistocene monsoon record from Hulu Cave, China, *Science*, 294, 2345–
534 2348, 2001a.

535 Wang, Y., Cheng, H., Edwards, R., He, Y., Kong, X., An, Z., Wu, J., Kelly, M., Dykoski, C.,
536 and Li, X.: The Holocene Asian monsoon: Links to solar changes and North Atlantic climate,
537 *Science*, 308, 854–857, 2005.

538 Wang, Y., Wang, B., Oh, J.: Impact of the preceding El Niño on the East Asian summer
539 atmosphere circulation, *J. Meteorol. Soc. Jpn.*, 79, 575-588, 2001b.

540 Wu, Z., Wang, B., Li, J., Jin, F.: An empirical seasonal prediction model of the east Asian
541 summer monsoon using ENSO and NAO, *J. Geophys. Res.*, 114, D181120, 2009.

542 Xu, H., Lan, J., Sheng, E., Liu, B., Yu, K., Ye, Y., Shi, Z., Cheng, P., Wang, X., Zhou, X., and
543 Yeager, K.: Hydroclimatic contrasts over Asian monsoon areas and linkages to tropical
544 Pacific SSTs, *Sci. Rep.*, 6, 33177, 2016.

545 Yan, H., Sun, L., Oppo, D., Wang, Y., Liu, Z., Xie, Z., Liu, X., and Cheng, W.: South China Sea
546 hydrological changes and Pacific Walker Circulation variations over the last millennium, *Nat.*
547 *Commun.*, 2, 293, 2011a.

548 Yan, H., Sun, L., Wang, Y., Huang, W., Qiu, S., and Yang, C.: A record of the Southern
549 Oscillation Index for the past 2,000 years from precipitation proxies, *Nat. Geosci.*, 4, 611-
550 614, 2011b.

551 Yan, H., Wei, W., Soon, W., An, Z., Zhou, W., Liu, Z., Wang, Y., and Carter, R.: Dynamics of
552 the intertropical convergence zone over the western Pacific during the Little Ice Age, *Nat.*
553 *Geosci.*, 8, 315, 2015.

554 Yu, R., Zhou, T.: Seasonality and Three-Dimensional Structure of Interdecadal Change in the
555 East Asian Monsoon, *J. Climate*, 20, 5344-5355, 2007.

556 Yuan, D., Cheng, H., Edwards, R., Dykoski, C., Kelly, M., Zhang, M., Qing, J., Lin, Y., Wang,
557 Y., Wu, J., Dorale, J., An, Z., and Cai, Y.: Timing, duration and transitions of the last
558 interglacial Asian monsoon, *Science*, 304, 575-578, 2004.

559 Zhang, H., Brahim, Y., Li, H., Zhao, J., Kathayat, G., Tian, Y., Baker, J., Wang, J., Zhang, F.,
560 Ning, Y., Edwards, R., Cheng, H.: The Asian Summer Monsoon: Teleconnections and
561 Forcing Mechanisms-A Review from Chinese Speleothem $\delta^{18}\text{O}$ Records, *Quaternary*, 2, 26,
562 2019.

563 Zhang, H., Cheng, H., Cai, Y., Spötl, C., Kathayat, G., Sinha, A., Edwards, R., Tan, L.:
564 Hydroclimatic variations in southeastern China during the 4.2ka event reflected by stalagmite
565 records, *Clim. Past*, 14, 1805-1817, 2018b.

566 Zhang, H., Cheng, H., Spötl, C., Cai, Y., Sinha, A., Tan, L., Yi, L., Yan, H., Kathayat, G., Ning,
567 Y., Li, X., Zhang, F., Zhao, J., Edwards, R.: A 200-year annually laminated stalagmite record
568 of precipitation seasonality in southeastern China and its linkages to ENSO and PDO, *Sci.*
569 *Rep.*, 8, 12344, 2018a.

570 Zhang, H., Griffiths, M., Chiang, J., Kong, W., Wu, S., Atwood, A., Huang, J., Cheng, H., Ning,
571 Y., Xie, S.: East Asian hydroclimate modulated by the position of the westerlies during
572 Termination I, *Science*, 362, 580-583, 2018c.

573 Zhang, P., Cheng, H., Edwards, R., Chen, F., Wang, Y., Yang, X., Liu, J., Tan, M., Wang, X.,
574 Liu, J., An, C., Dai, Z., Zhou, J., Zhang, D., Jia, J., Jin, L., and Johnson, K.: A test of climate,
575 sun, and culture relationships from an 1810-year Chinese cave record, *Science*, 322, 940-
576 942, 2008.

577 Zhang, W., Chen, S., Wang, Y., Zhao, K., Shao, Q., Wang, T., and Zhu, L.: Rapid changes in the
578 East Asian summer monsoon: stalagmite records in Hubei, China, *Quaternary Sci.*, 39, 765-
579 774, 2019 (in Chinese with English abstract).

580 Zhao, K., Wang, Y., Edwards, R., Cheng, H., and Liu, D.: High-resolution stalagmite $\delta^{18}\text{O}$
581 records of Asian monsoon changes in central and southern China spanning the MIS3/2
582 transition, *Earth Planet Sci. Lett.*, 298, 191–198, 2010.

583 Zhao, K., Wang, Y., Edwards, R., Cheng, H., Liu, D., and Kong, X.: A high-resolved record of
584 the Asian Summer Monsoon from Dongge Cave, China for the past 1200 years, *Quaternary*
585 *Sci. Rev.*, 122, 250-257, 2015.

586 Zhao, K., Wang, Y., Edwards, R., Cheng, H., Liu, D., Kong, X., and Ning, Y.: Contribution of
587 ENSO variability to the East Asian summer monsoon in the late Holocene, *Palaeogeogr.*
588 *Palaeoclimatol.*, 449, 510-519, 2016.

589 Zhou, T., Gong, D., Li, J., Li, B.: Detecting and understanding the multi-decadal variability of
590 the East Asian Summer Monsoon-Recent progress and state of affairs, *Meteorol. Z.*, 13, 455-
591 467, 2009.

592

593 **Table and figure**

594

595 Table 1 U-series dating results of stalagmite YX262 from Yongxing Cave

596

Sample depth (mm)	^{238}U (ppb)	^{232}Th (ppt)	$\delta^{234}\text{U}$ (measured)	$^{230}\text{Th}/^{238}\text{U}$ (activity)	^{230}Th Age (a) (uncorrected)	$\delta^{234}\text{U}_{\text{initial}}$ (corrected)	^{230}Th Age (a) (corrected)
YX262-5	546.0±0.5	307.9±0.6	607.5±1.0	0.006230157±0.00014	423.5±9.4	608.2±1.0	413.1±10.8
YX262-25	595.5±0.3	280.5±0.6	790.6±1.9	0.00788248±0.00008	481.0±5.1	791.7±1.9	473.1±6.3
YX262-48	506.3±0.3	281.6±0.5	762.1±1.9	0.009468079±0.00010	587.3±6.4	763.4±1.9	577.9±8.0
YX262-75	517.7±0.3	724.3±0.1	680.5±2.1	0.010930422±0.00010	711.3±6.4	681.8±2.1	686.3±13.9
YX262-95	651.8±0.3	1448.0±0.3	806.5±2.0	0.013146471±0.00010	796.0±6.3	808.3±2.0	759.4±19.1
YX262-116	583.4±0.8	283.0±0.4	956.6±1.0	0.014987259±0.00012	838.0±6.6	958.9±1.0	830.8±7.5

597 Decay constant values are $\lambda_{234}=2.82206\times 10^{-6}\text{a}^{-1}$, $\lambda_{238}=1.55125\times 10^{-10}\text{a}^{-1}$, $\lambda_{230}=9.1705\times 10^{-16}\text{a}^{-1}$ and $\delta^{234}\text{U} =$
598 $(\frac{^{234}\text{U}}{^{238}\text{U}})_{\text{activity}}-1)\times 1000$. Corrected ^{230}Th age calculation, indicated in bold, is based on an assumed initial
599 $^{230}\text{Th}/^{232}\text{Th}$ atomic ratio of $(4 \pm 2) \times 10^{-6}$. All corrected dates are years before 2017 A.D.

600

601

602

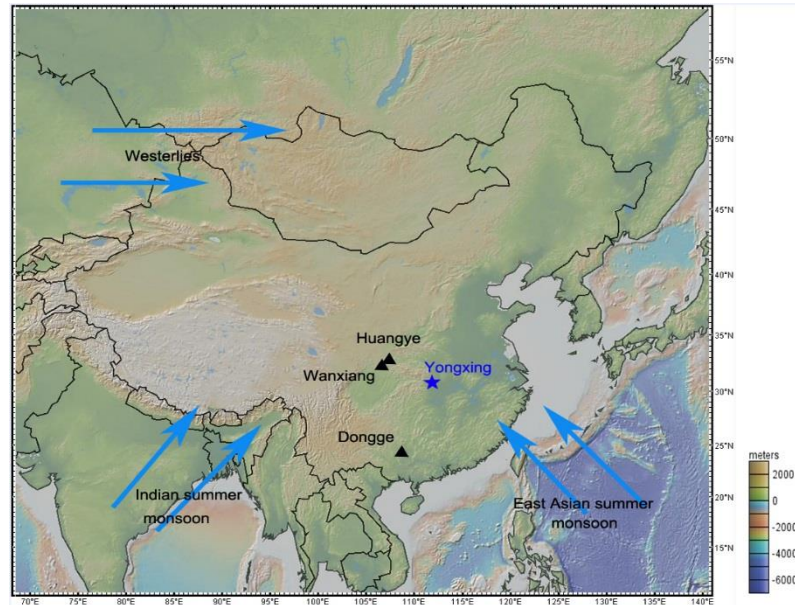
603

604

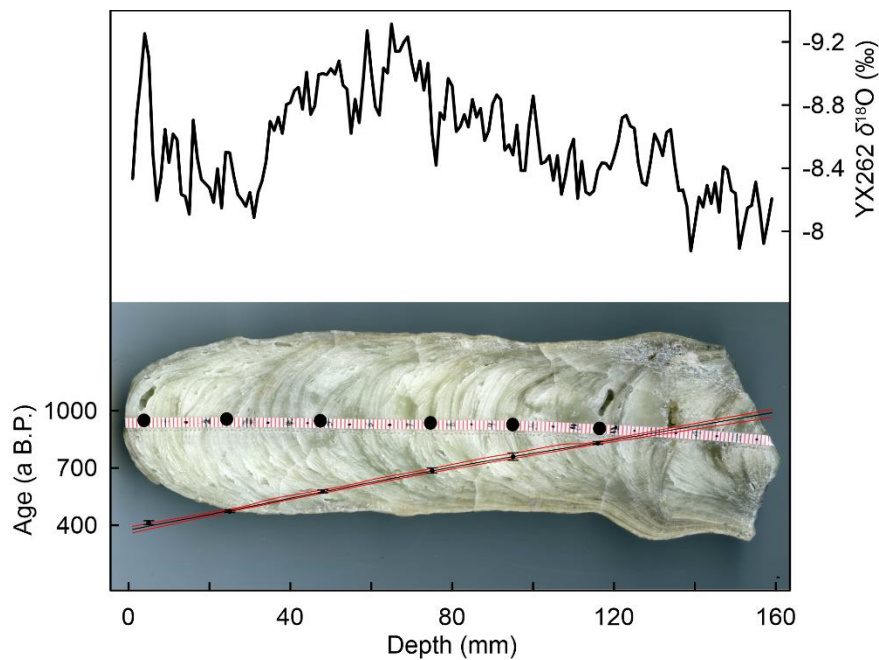
605

606

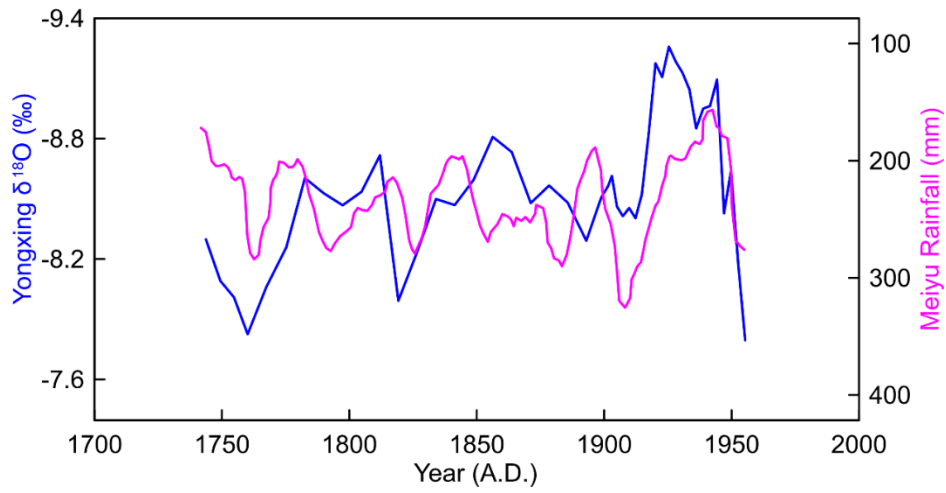
607
608
609
610
611
612
613
614
615
616
617
618
619



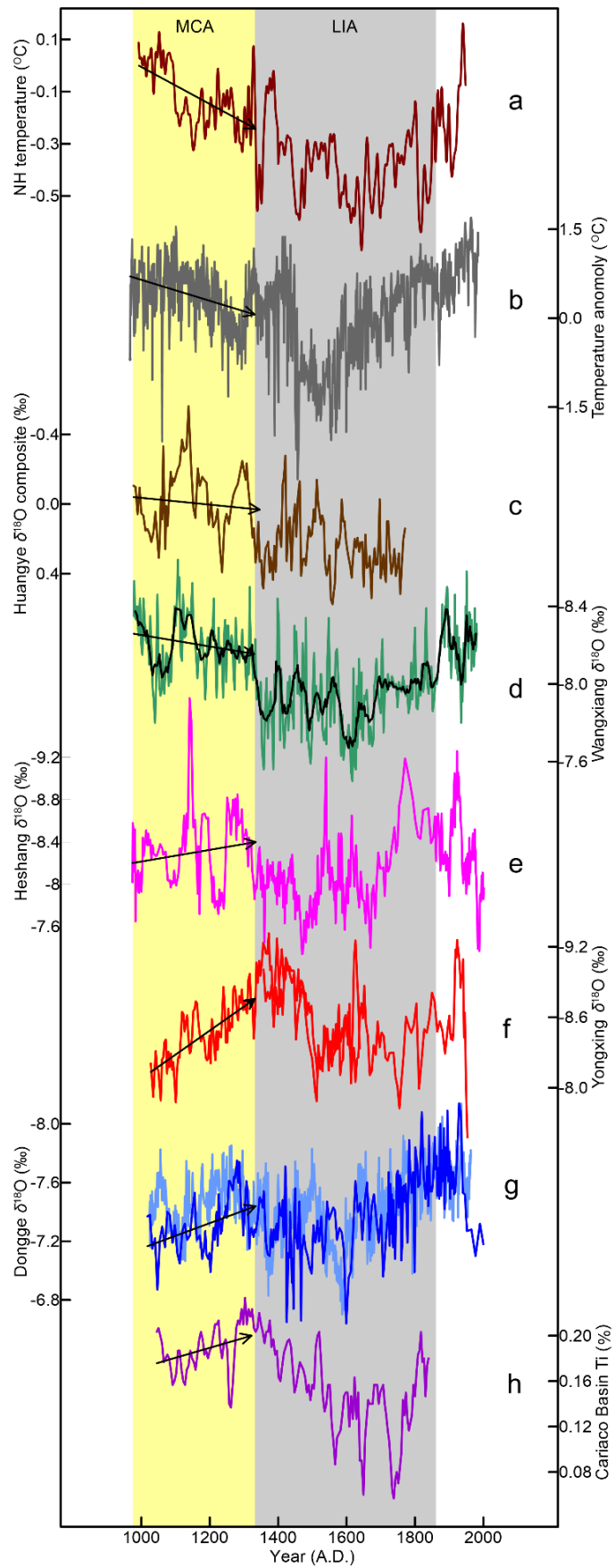
620 Fig.1 Schematic climate setup of East Asian Monsoon and our study site. The blue star
621 and black triangles represent Yongxing Cave in central China and other caves in the
622 monsoonal region, respectively.



623 Fig. 2 The age versus depth model, image and $\delta^{18}\text{O}$ record for our stalagmite YX262.
624 The small black dots and vertical error bars indicate ^{230}Th dates and errors of these
625 dates, respectively. The big black dots represent the locations of ^{230}Th dates. The middle
626 green line indicates the model age, and upper and lower red lines indicate the age in 95%
627 confidence level, respectively.



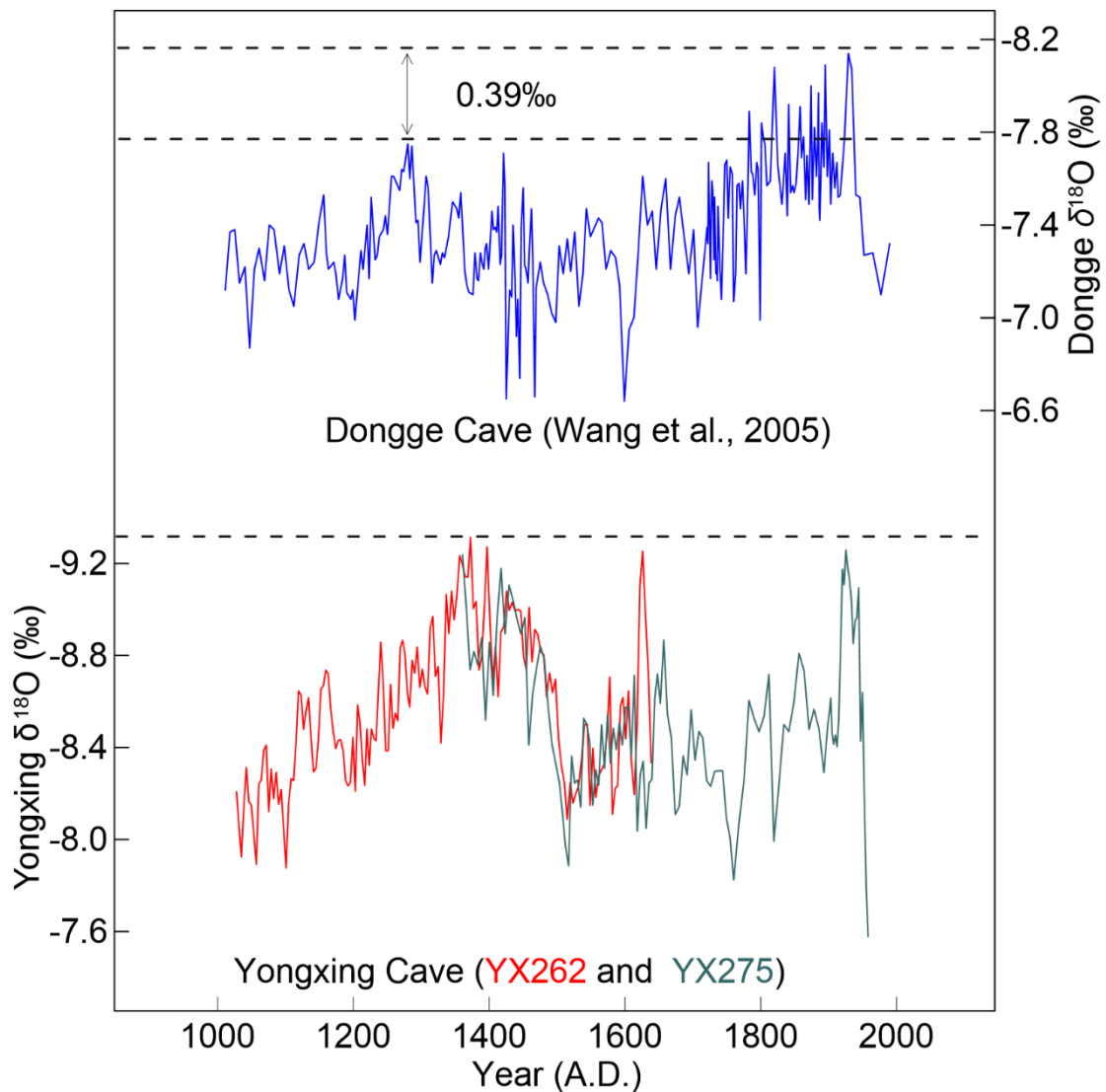
629 Fig.3 A comparison between the Yongxing $\delta^{18}\text{O}$ record (blue line) and reconstructed
630 Meiyu rain (pink line; 7-years running average; Ge et al., 2008).



631

632 Fig. 4 A comparison of the Yongxing $\delta^{18}\text{O}$ time-series with other proxy records. (a)

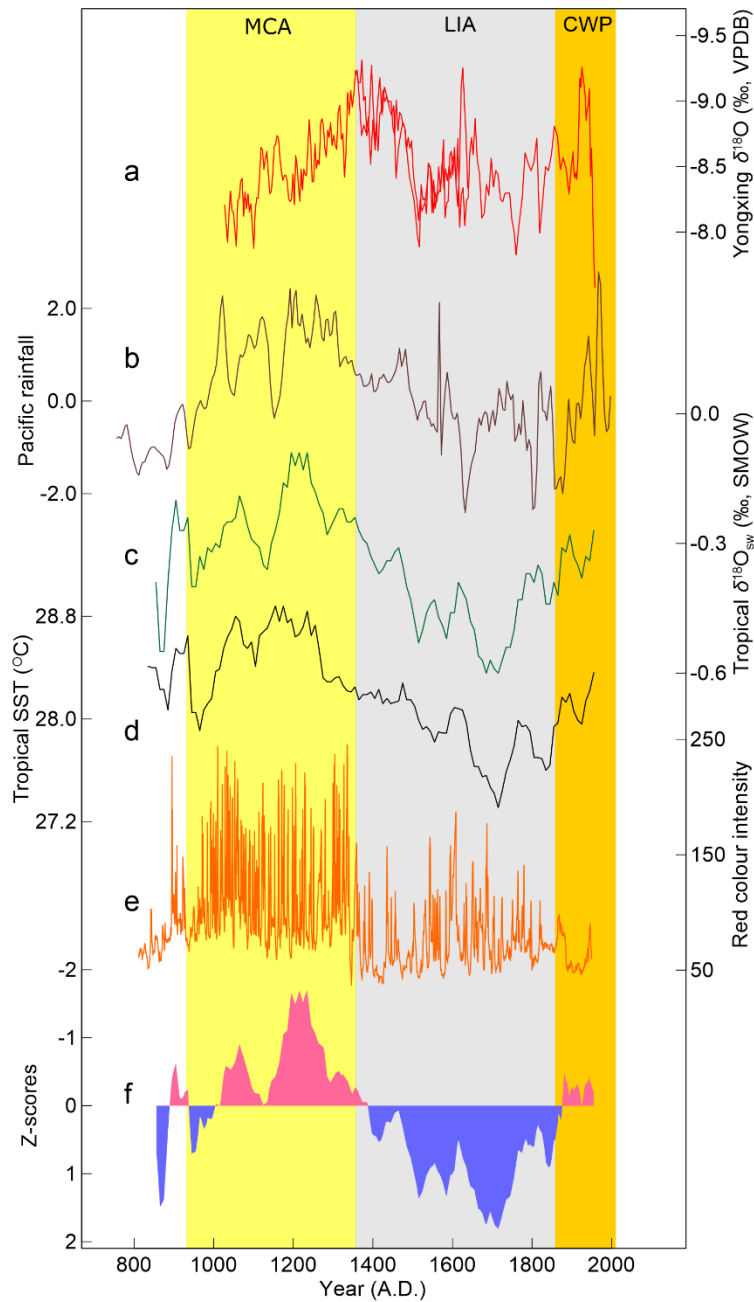
633 Northern Hemisphere reconstructed temperature (Mann et al., 2009); (b) Northern
 634 China reconstructed temperature (Tan et al., 2003); (c) Huangye Cave $\delta^{18}\text{O}$ composite
 635 (Tan et al., 2011); (d) Wanxiang Cave $\delta^{18}\text{O}$ record (Zhang et al., 2008); (e) Heshang
 636 Cave $\delta^{18}\text{O}$ record (Hu et al., 2008); (f) Yongxing Cave record (this study); (g) Dongge
 637 Cave record (Wang et al., 2005; Zhao et al., 2015); (h) Cariaco Basin Ti content record
 638 (Haug et al., 2001). Light yellow and blue bars indicate the MCA and LIA, respectively.
 639 Arrows, constrained by linear fit methods, indicate trends of the climatic variations.
 640
 641



642
 643

644 Fig. 5 The relative intensity of Meiyu rain during the MCA as compared to the CWP.
 645 The upper panel is the Dongge cave record (blue curve, Wang et al., 2005); the lower
 646 panel is the Yongxing Cave YX262 (red curve) and YX275 (green curve, Zhang W et
 647 al., 2019) records. On average, the Dongge Cave record shows a 0.39‰ lower $\delta^{18}\text{O}$
 648 value during the CWP than the MCA. However, the Yongxing record shows a
 649 comparable value between the CWP and MCA.
 650

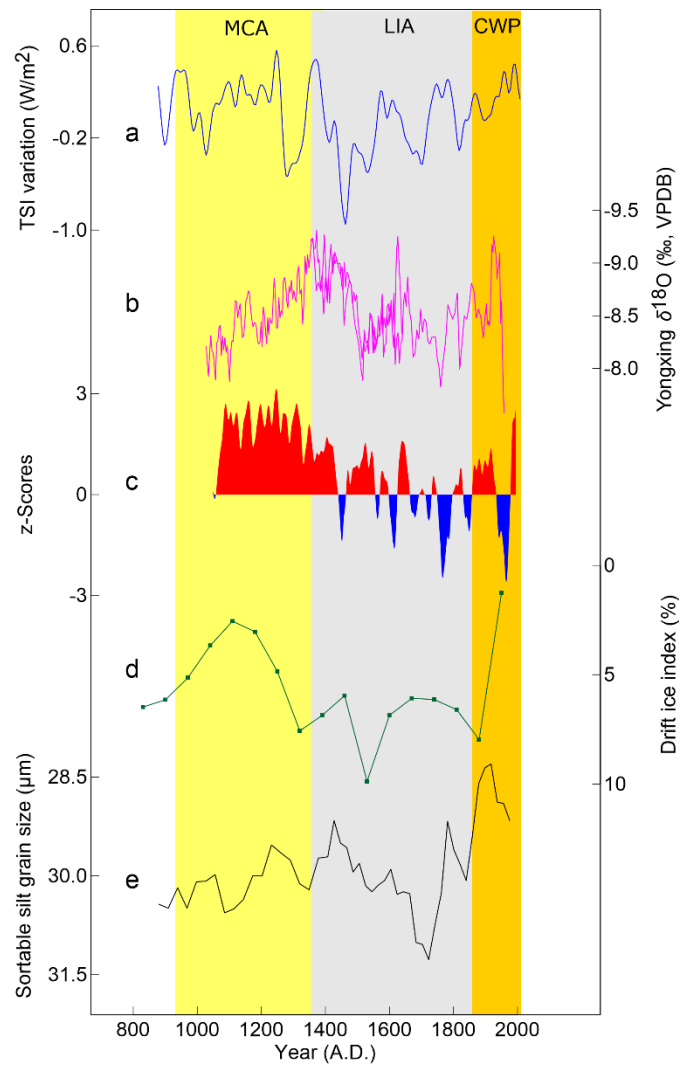
651
 652
 653
 654
 655
 656
 657
 658
 659
 660
 661
 662
 663
 664
 665
 666
 667
 668
 669
 670
 671
 672
 673
 674
 675
 676
 677
 678
 679
 680
 681
 682



683 Fig. 6 A comparison between Meiyu rain and Pacific climate. (a) Yongxing cave record
 684 (this study); (b) Tropical Pacific rainfall record (Oppo et al., 2009); (c) Tropical Pacific
 685 $\delta^{18}\text{O}$ record (Oppo et al., 2009); (d) Tropical Pacific sea surface temperature (Oppo et
 686 al., 2009); (e) Red colour intensity in southern Ecuador (Moy et al., 2002); (f)
 687 Hydrological reconstruction of ENSO from Tropical Pacific (Yan et al., 2011a). Yellow,
 688 grey and orange bands represent the MCA, LIA, and CWP, respectively.

689
 690
 691
 692
 693
 694

695
696
697
698
699
700
701
702
703
704
705
706
707
708
709
710
711
712
713
714
715
716
717
718
719
720
721



722 Fig. 7 A comparison among Meiyu rain, solar activity and North Atlantic climate. (a)
723 Total solar irradiance (Steinhilber et al., 2009); (b) Yongxing Cave record (this study);
724 (c) North Atlantic Oscillation index (Trouet et al., 2009); (d) North Atlantic drift ice
725 index (Bond et al., 2001); (e) Sortable silt grain size in the North Atlantic (Thornalley
726 et al., 2018). Yellow, grey and orange bands represent the MCA, LIA, and CWP,
727 respectively.
728